Author Manuscript

Author Manuscript

Author Manuscript

Author Manuscript

HHS Public Access

Author manuscript

Mol Cell. Author manuscript; available in PMC 2019 May 17.

Published in final edited form as:

Mol Cell. 2018 May 17; 70(4): 679–694.e7. doi:10.1016/j.molcel.2018.04.014.

SRC-3 coactivator governs dynamic estrogen-induced chromatin looping interactions during transcription

Anil K. Panigrahi[1], **Charles E. Foulds**[1,2], **Rainer B. Lanz**[1], **Ross A. Hamilton**[1], **Ping Yi**[1], **David M. Lonard**[1], **Ming-Jer Tsai**[1], **Sophia Y. Tsai**[1], and **Bert W. O'Malley**[1,*]

[1]Department of Molecular and Cellular Biology, Baylor College of Medicine, One Baylor Plaza, Houston, TX 77030, USA

[2]Center for Precision Environmental Health, Baylor College of Medicine, One Baylor Plaza, Houston, TX 77030, USA

SUMMARY

Enhancers are thought to activate transcription by physically contacting promoters via looping. However, direct assays demonstrating these contacts are required to mechanistically verify such cellular determinants of enhancer function. Here, we present versatile cell-free assays to further determine the role of enhancer-promoter contacts (EPC). We demonstrate that EPC is linked to mutually stimulatory transcription at the enhancer and promoter in vitro. SRC-3 was identified as a critical looping determinant for the estradiol-(E2)-regulated *GREB1* locus. Surprisingly, the *GREB1* enhancer and promoter contact two internal gene-body SRC-3 binding sites, GBS1 and GBS2, which stimulate their transcription. Utilizing time-course 3C assays, we uncovered SRC-3 dependent dynamic chromatin interactions involving the enhancer, promoter, GBS1, and GBS2. Collectively, these data suggest that the enhancer and promoter remain 'poised' for transcription via their contacts with GBS1 and GBS2. Upon E2 induction, GBS1 and GBS2 disengage from the enhancer, allowing direct EPC for active transcription.

ETOC BLURB

Panigrahi et al. present versatile cell-free assays for measuring enhancer-promoter contacts and transcription that identified SRC-3 as a looping determinant for estrogen (E2)-responsive genes. E2 instigates SRC-3-dependent dynamic chromatin interactions at target genes, where SRC-3-bound intronic sequences dissociate from the enhancer to allow direct enhancer-promoter contact required for transcription activation.

[*]Lead contact to whom correspondence should be addressed. Tel: +1 713 798 6205; Fax: +1 713 798 5599; berto@bcm.edu.

Publisher's Disclaimer: This is a PDF file of an unedited manuscript that has been accepted for publication. As a service to our customers we are providing this early version of the manuscript. The manuscript will undergo copyediting, typesetting, and review of the resulting proof before it is published in its final citable form. Please note that during the production process errors may be discovered which could affect the content, and all legal disclaimers that apply to the journal pertain.

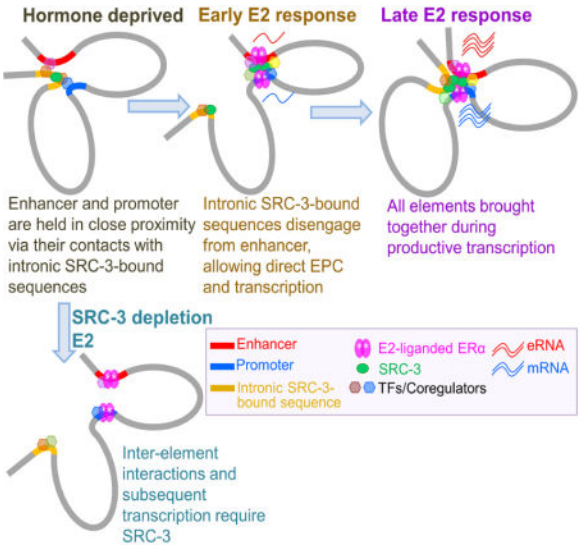
AUTHOR CONTRIBUTIONS

A.K.P. and B.W.O. designed research, B.W.O. directed the study; A.K.P. performed most experiments, analyzed the results, and was the primary author of the manuscript; C.E.F. and R.B.L. contributed technical help; R.A.H. provided nuclear extracts; P.Y. provided recombinant SRC-3; M.-J.T., S.Y.T., and D.M.L. shared ideas. A.K.P., C.E.F., R.B.L., M.-J.T., S.Y.T., D.M.L. and B.W.O. revised the paper.

DECLARATION OF INTERESTS

The authors declare no competing interests.

Author Manuscript Author Manuscript Author Manuscript Author Manuscript



Keywords

Enhancer-promoter interaction; looping determinant; estrogen receptor-α (ERα); Steroid Receptor Coactivator-3 (SRC-3); estrogen-induced transcription

INTRODUCTION

RNA polymerase II (RNA pol II) transcribed genes are activated by regulatory DNA sequence elements known as enhancers that act in *cis* over long distances (Banerji et al., 1981; Heuchel et al., 1989). Enhancers are evolutionarily conserved in sequence and function (Visel et al., 2009), contain dense clusters of transcription factor (TF) binding sites (Spitz and Furlong, 2012) and are heavily occupied by TFs, coactivators, cohesin, the mediator complex, RNA polymerase II (RNA Pol II) and chromatin regulatory enzymes (Liu et al., 2014; Malik and Roeder, 2016; Yan et al., 2013), and exhibit specific chromatin features (Rada-Iglesias et al., 2011). When bound by TFs and brought into proximity of their cognate promoters, the enhancers stimulate transcription of their target genes (Blackwood and Kadonaga, 1998; Marsman and Horsfield, 2012; Ptashne, 1986) and undergo transcription to produce enhancer RNAs (eRNAs) (Li et al., 2016).

Enhancer-promoter pairs in contact over long distances have been identified using the chromosome conformation capture (3C) technique and its derivatives (Denker and de Laat, 2016; Ong and Corces, 2011; Spurrell et al., 2016). Such studies have revealed several important features of enhancer function: (1) pervasive enhancer-promoter contacts (EPCs) exist throughout the genome resulting from looping between distant chromatin segments (Jin et al., 2013; Zhang et al., 2013). (2) Pre-formed EPCs exist at transcriptionally inert loci in the absence of any transcriptional stimulus (Andrey et al., 2013; Ghavi-Helm et al., 2014; Jin et al., 2013; Phanstiel et al., 2017) and are thought to keep the gene loci ‘poised’ for transcription. (3) EPCs can form *de novo* upon transcriptional stimulation (Fullwood et al., 2009; Hah et al., 2013; Li et al., 2013) or upon the availability of the key TFs (Vakoc et al., 2005). Both pre-formed and *de novo* EPCs participate in transcriptional regulation (Phanstiel

Author Manuscript Author Manuscript Author Manuscript Author Manuscript

et al., 2017). (4) EPC is required for efficient transcription from a participating promoter (Deng et al., 2012). (5) However, maintenance of EPC is not dependent on active transcription (Palstra et al., 2008). (6) Several classes of coregulators contribute to EPC establishment, such as tissue-specific TFs (Vakoc et al., 2005; Yun et al., 2014), the cohesin complex (Hadjur et al., 2009; Kagey et al., 2010; Schmidt et al., 2010), the mediator complex (Kagey et al., 2010; Malik and Roeder, 2016), specialized 'bridging' factors (Chen et al., 2012; Krivega et al., 2014; Ren et al., 2011), and chromatin remodelers like SWI/SNF and NuRD (Euskirchen et al., 2011; Krivega et al., 2014). (7) EPC also has been implicated in transcriptional pause release of genes regulated by a subset of JMJD6 and BRD4-bound enhancers (Liu et al., 2013). (8) Additionally, an enhancer-silencer contact can prevent EPC formation, leading to gene repression (Jiang and Peterlin, 2008).

Although these studies have provided important information on enhancers and their interactions with cognate promoters, our full mechanistic understanding of enhancer function remains incomplete. Addressing the specific mechanistic and functional implications of EPC in living cells has been challenging due to the complexity and dynamic nature of the cellular environment. Therefore, we developed new and highly controllable cell-free assays for EPC that are capable of interrogating transcriptional and proteomic dynamics in vitro. Here, we show that the classical Dignam HeLa cell nuclear extract (Dignam et al., 1983) promotes EPC in vitro, which is further enhanced when transcription ensues at both enhancer and promoter. We identified the steroid receptor coactivator-3 (SRC-3, NCOA3) as a critical and novel determinant of looping in both our cell free systems and in intact MCF-7 cells that enables dynamic chromatin interactions at the human *GREB1* gene. In E2-depleted MCF-7 cells, we find that the enhancer holds the promoter in close proximity via direct contacts with SRC-3 binding sites located downstream from the *GREB1* transcription start site (TSS). Upon E2 treatment, this connection is reorganized rapidly, leading to a temporal sequence of enhancer-promoter-intragenic looping contacts. Additionally, these gene-body SRC-3 binding sites were found to be necessary for efficient transcription both at enhancer (eRNA) and promoter (mRNA) in vitro. We also present evidence that both formation and severance of chromatin interaction contacts are crucial for full transcriptional activity. We demonstrate that our looping assay is versatile, which can successfully recapitulate serum-inducible EPC and transcription activation in vitro.

RESULTS

Development of novel looping assays to interrogate enhancer-promoter contact in vitro

To investigating EPC at a mechanistic level, we developed several cell-free methodologies. We chose the human *GREB1* locus as a looping model because the *GREB1* gene undergoes E2-inducible EPC in MCF-7 cells that correlates with its strong activation (Fullwood et al., 2009; Hah et al., 2013; Li et al., 2013). The *GREB1* enhancer was identified 41 kb upstream of the major transcription start site (TSS; *GREB1c* isoform) based on the magnitude of E2-induced ERα occupancy, ERα-anchored interaction with the promoter, enrichment of H3K4me1 and H3K27ac, as well as the magnitude of E2-induced eRNA synthesis (Fullwood et al., 2009; Hah et al., 2013; Li et al., 2013). Interspersed between the enhancer and the *GREB1c* promoter are three estrogen response elements (EREs) (Sun et al., 2007)

Author Manuscript Author Manuscript Author Manuscript Author Manuscript

that do not share the above characteristics of the enhancer. An additional ERα-bound region ERE1^{up} (Figure S1A) also exhibits ERα-mediated contact with the enhancer (Fullwood et al., 2009). We designed a compact DNA construct that contained all these elements and the *GREB1c* promoter, while removing selected intervening DNA. We PCR-amplified these elements (Figures 1A and S1A), and verified by DNA pulldown assays (Foulds et al., 2013) that ERα binds each of these fragments and recruits coregulators, including SRC-3, RAD21, MED12 and CDK8, from HeLa S3 nuclear extract (HeLa NE) (Figure S1B). These six regulatory fragments, named F1-F6, were then assembled into an 8 kb composite fragment, named CompF (Figure 1A).

We reasoned that if EPC occurred on the CompF, F6 would still be retained with F1 even after it is cleaved from the rest of the template with a restriction enzyme (Figure 1B). To test this possibility, we immobilized 5′biotinylated CompF on M280 streptavidin-coated Dynabeads, and incubated it with HeLa NE as a source of potential looping factors, along with recombinant ERα protein and ATP. HeLa NE was chosen because it lacks endogenous ERα (Figure S1B; (Foulds et al., 2013)), allowing us to control the availability of the key regulator of *GREB1* expression. The bound complexes were digested with *Sac*I to cleave off F6 (Figure 1B; Figure S1C). The beads were washed again, and both F6 and F1 were quantified in the remaining bound fraction by quantitative PCR (qPCR). Parallel reactions were carried out with the doubly biotinylated CompF (DBiot.CompF, biotinylated at both 5′ and 3′ ends). By comparing the amount of F6 retention on both 5′Biot. and DBiot.CompF, we were able to calculate the fraction of F6 retained, which we call the ‘looping index’. We observed HeLa NE-dependent retention of F6 with F1 that further increases in the presence of ERα (Figure 1C). We carried out a similar “Looping assay” with MCF-7 NE and E2, which revealed that ligand-activated ERα is required for maximal loop formation (Figure S1D).

EPC can locally be viewed as an interaction in *trans* (Figure S1E). Thus, conceptually, a biotinylated enhancer fragment should be able to capture an unbiotinylated promoter fragment, and *vice versa* (Figure S1F). We tested this possibility in our *trans*-interaction assay performed under identical conditions as described above. Biotinylated F1 (Biot. F1) was first immobilized on M280 beads and then incubated with unbiotinylated F6, HeLa NE, ATP and ERα. After washes, we quantified F6 enrichment in the bound fractions relative to Biot.F1 using qPCR, which gave a measure of EPC or ‘*trans*-Interaction index’ (Figure 1D). Consistent with the looping assay above, we observed strong F1-F6 interaction in the presence of HeLa NE, which is significantly enhanced by ERα. Importantly, F2 and F3 did not interact with Biot.F1, whereas F4 and F5 displayed a very modest interaction with Biot. F1 (Figure S1G), indicating F1-F6 interaction specificity. The *trans*-Interaction assay with MCF-7 NE revealed E2-enhanced F1-F6 interaction (Figure S1H). Chromatinized F1 and F6 fragments interacted with comparable efficiency as seen with ‘naked’ DNAs (Figure S1I, S1J).

Next, to make our assay more physiologically-relevant, we investigated whether EPC would occur on a BAC clone of the *GREB1* locus that contains ‘all intervening sequences’. Conceptually, EPC on the BAC clone should be detectable using an approach based on the conventional chromosome conformation capture (3C) assay (Figure S1K). We developed an

Author Manuscript Author Manuscript Author Manuscript Author Manuscript

in vitro 3C (IV3C) assay using the BAC clone CTD-3138J7 as a template, while keeping the reaction conditions identical to the looping assays described above. The reactions were crosslinked with formaldehyde, purified over a spin column, digested with *PstI*, diluted 20-fold, ligated, purified, and the ligants (ligated fragments) were quantified by qPCR (Figure S1L details the relative locations of *PstI* sites and the 3C primers). The resulting values reflected the magnitude of inter-fragment crosslinking, called 'Looping Index^{IV3C}'. To examine EPC in the context of transcription, we interrogated the enhancer's contact with both upstream ("preTSS", a *PstI* site 1.6 kb upstream of the TSS) and downstream ("postTSS", a *PstI* site 1 kb downstream of TSS) regions of the promoter (Figure S1L). Both of these contacts increase in the presence of ERα, while no contact of the enhancer with a control sequence near F2 was detected (Figure 1E). We were unable to conduct IV3C on a chromatin template as we could not reconstitute the BAC into chromatin. We detected similar E2-induced enhancement of Enh-preTSS and Enh-postTSS contacts when we conducted the IV3C with MCF-7 NE (Figure S2A). We also conducted IV3C on a BAC clone (RP11-1025G18) harboring the *NRIP1* gene, which revealed both Enh-preTSS and Enh-postTSS contacts in presence of HeLa NE and ERα (Figure S2B), similar to *GREB1*.

The high EPC detected in our assays in the absence of ERα could potentially reflect non-specific contacts. To test this, we conducted looping assay and *trans*-Interaction assay with YY1-immunodepleted HeLa NE (YY1 likely mediates pre-formed EPCs (Weintraub et al., 2017)). Interestingly, YY1 depletion significantly lowered background EPC (NE only), whereas ERα-mediated EPC was unaffected (Figure S2C), suggesting that a significant proportion of the background EPC in vitro is YY1-regulated and, therefore, physiologically relevant.

To test the versatility of our assay system, we prepared NE from HeLa cells serum-starved for 48 hours and after 2 hours of serum stimulation. We used BAC clone CTD-2655F5, harboring the classical serum-inducible gene *FOS* to interrogate serum-inducible EPC in vitro. As the IV3C data in Figure 1F reveal, the two flanking enhancers Enh1 and Enh2 made contacts with the promoter and with themselves in the presence of the NE prepared from serum-starved cells (Starved). Interestingly, we observed 2-3 fold higher Looping Index^{IV3C} for these contacts in the presence of NE prepared from serum-stimulated cells (+FBS; Figure 1F). The enhancers and the promoter did not contact a control region (Ctr) in this assay. Importantly, these same contacts are observed in 3C assays in HeLa cells similarly serum-starved and FBS-stimulated validating the above data (Figure S2D).

Taken together, we developed novel cell-free methodologies, which demonstrate that HeLa cell nuclear extracts made using a standard protocol (Dignam et al., 1983) can facilitate EPC and that these contacts can be enhanced by signal-dependent TFs (e.g., ERα and serum-responsive TFs).

EPC in vitro corresponds with transcription activation

Since EPC has been linked with transcription activation, we expected stronger EPC in vitro under conditions that support transcription. To test this, we first examined if our CompF template could support enhancer and activator-dependent stimulation of promoter-driven transcription. We conducted in vitro transcription (IVT) on CompF as well as CompFΔF1,

Author Manuscript Author Manuscript Author Manuscript Author Manuscript

which lacked the enhancer. The IVT reaction conditions were essentially the same as the other looping assays, except that the reactions were shifted to 30°C after addition of 0.5 mM NTPs to allow transcription. Figure 2A demonstrates ERα-dependent activation of *GREB1* promoter-driven transcription, mRNA, in vitro (and also eRNA; see Figure S2E). This activation is enhancer-dependent, as ERα failed to activate mRNA synthesis on CompFΔF1. These results reveal that the reaction conditions required for EPC also are optimal for transcription activation in vitro. Importantly, the CompF exhibited a strong looping index under transcription-permissive conditions (+NTPs, 30°C), while the CompFΔF1 also failed to exhibit F6 retention in the looping assay (Figure 2B). This result demonstrates that the *GREB1* promoter (F6) loops to the enhancer (F1), but not to intervening regions F2-F5.

Next, we examined various cell-free requirements for EPC vis-à-vis transcription activation. We set up the looping assay with CompF and the reactions were processed for both looping readout and quantitation of transcription (Figures 2C and 2D, respectively). Again, EPC is dependent on the presence of NE and is enhanced by the co-addition of ERα and ATP. However, when NTPs were added followed by incubation at 30°C ('transcription' condition), we detected maximal EPC (Figure 2C). Interestingly, we detected maximal production of both eRNA and mRNA under this condition (Figure 2D). Similar patterns of EPC enhancement by ERα under transcription conditions were observed in *trans*-interaction and IV3C assays (Figures 2E and 2F, respectively). We detected maximal eRNA and mRNA production in vitro at *GREB1*, *NRIP1* and *FOS* loci with their respective BAC clones under conditions that generate optimal EPC (Figures S2F, S2G, and S2H, respectively).

Interestingly, the enhancer's contact with the post-TSS region of the promoter weakens under these conditions (Figure 2F), possibly suggesting that efficient formation of the pre-initiation complex (PIC) and subsequent re-initiation cycles of transcription might require stronger contact between the enhancer and the pre-TSS promoter, while the post-TSS region disengages from the enhancer, possibly to allow facilitated passage of the elongating RNA Pol II complex. Collectively, these results reveal that EPC establishment in vitro by NE requires ATP and ERα, and maximal EPC is achieved under conditions of maximal activated transcription. Importantly, EPC appears to undergo dynamic changes after the induction of transcription, as suggested by differences in enhancer-preTSS and enhancer-postTSS interactions.

Mutual co-stimulation of enhancer and promoter transcription in vitro

The maximal *trans*-interaction between the enhancer and promoter fragments achieved under 'transcription' condition (Figure 2E) prompted us to ask if the individual fragments transcribe under these conditions—since these regions are efficiently transcribed under the same conditions as part of the CompF (Figure 2D) and the BAC clone (Figure S2F). Interestingly, F1 and F6 fragments individually did not transcribe very well, and ERα failed to sufficiently activate their transcription. However, both fragments transcribed efficiently when present in the reaction together (templates F1+F6, Figure 2G; identical to *trans*-interaction under 'transcription' condition). This phenomenon was specific to the enhancer-promoter combination, since F2 and F3 failed to elicit such transcriptional induction (Figure

Author Manuscript Author Manuscript Author Manuscript Author Manuscript

S2I). Taken together with the trans-interaction results, this observation indicates a critical role of EPC in establishing mutual transcription activation from each other.

Since eRNAs have been proposed to activate promoter transcription, we tested for a possible role of the enhancer and promoter transcripts in mutual transcription activation. In IVT reactions, we incubated F1 with promoter-derived synthetic mRNA, and F6 with enhancer-derived synthetic eRNA. Interestingly, the synthetic eRNA and mRNA failed to elicit transcription activation at the promoter and enhancer, respectively (Figure 2H). This result suggests that mutual co-stimulation of transcription at an enhancer and promoter is "co-transcriptional" and not dependent on the actual transcripts *per se*. Supplemental mRNA and eRNA failed to stimulate transcription at enhancer and promoter, respectively, in an IVT reaction with CompF.

SRC-3 is a critical looping determinant

We next sought to identify protein factors that function as looping determinants. As the mediator complex and cohesin have been proposed to contribute to EPC (Kagey et al., 2010; Malik and Roeder, 2016), we first verified their requirement for EPC promotion in our assays. Immuno-depletion of either complex reduced EPC by over 50% in our *trans*-Interaction assay (Figure 3A, Figure S3A), while the loss of HDAC1 did not impact looping.

ERα transcriptional activation depends on the p160-family of coactivators SRC-1, SRC-2 and SRC-3 (Acevedo et al., 2004; Shang et al., 2000). Also, SRC-3 serves as a primary platform that recruits other coactivators such as CBP and p300 to ERα-bound sequences, and plays an essential role in mediating ERα activity (Foulds et al., 2013; Yi et al., 2015). Therefore, we next examined if SRC-3 depletion would affect EPC. Loss of SRC-3 from immunodepleted HeLa NE significantly reduced EPC in our *trans*-Interaction, looping and IV3C assays (Figures 3B, 3C and 3D, respectively). Depletion of SRC-1 and SRC-2 had only a modest effect on EPC when compared to SRC-3 (Figure S3B).

To verify the importance of SRC-3 for EPC in ERα-expressing cells, we conducted 3C-qPCR after SRC-3 knockdown in MCF-7 cells and analyzed the crosslinked contacts the same way as for our IV3C assay. The resulting values reflect the crosslinking efficiency, and are referred to as the 'Looping Index^{3C}' (Figure 3E). As in IV3C, we observed E2-dependent contact of the enhancer with both preTSS and postTSS regions of the promoter. However, these interactions greatly diminished in cells transfected with siRNAs targeting SRC-3 (Figure 3E). As reported earlier, ERα is required for EPC at the *GREB1* locus (Fullwood et al., 2009); our results suggest that this function of ERα strongly relies on SRC-3. EPC at the *TFF1* (Figure S3C) and *NRIP1* (Figure S3D) loci also similarly diminished upon SRC-3 depletion. We verified that SRC-3 was efficiently knocked down both at the protein and mRNA levels (Figures S3E, S3F).

To validate the importance of SRC-3 in EPC, we supplemented our IV3C reactions with recombinant wild type (WT) SRC-3 as well as a mutant deficient in interacting with coactivators such as p300 (ΔCID; (Yi et al., 2015); Figure S3H). The WT SRC-3 partially rescued the looping defect in vitro, whereas the ΔCID mutant failed to do so (Figure 3F). When we performed IVT with immunodepleted HeLa NE, we observed a reduction in ERα-

Author Manuscript Author Manuscript Author Manuscript Author Manuscript

activated transcription (both eRNA and mRNA) on the *GREB1* BAC template upon loss of SRC-3; this effect was partially rescued by addition of WT SRC-3, but not the ΔCID mutant to the reaction (Figure 3G). The inability of WT SRC-3 to fully rescue looping and transcription defect may stem from loss of associated p300 during SRC-3 immuno-depletion (Figure S3I). The transcription defect in ΔSRC-3 HeLa NE in vitro is in agreement with attenuated E2-inducible activation of *GREB1*, *TFF1* and *NRIP1* genes upon SRC-3 knockdown in MCF-7 cells (Figure S3G; (Won Jeong et al., 2012)).

RNA Pol II recruitment to the enhancer-promoter combination was clearly reduced in the absence of SRC-3, both with and without ERα, as seen in a F6-Biot.F1 combination pulldown followed by immunoblotting (Figure 3H). This could potentially explain defective EPC and transcription in ΔSRC-3 HeLa NE. These results collectively indicate that SRC-3 plays an important role in transcriptional activation both by establishing EPC and by promoting RNA Pol II recruitment.

The *GREB1* enhancer makes long range contacts beyond the promoter

Previously, we reported SRC-3 occupancy at E2-inducible enhancers and promoters, which further increased upon E2-induction (Lanz et al., 2010). Remarkably, we also observed strong intragenic SRC-3 binding, particularly within introns. These observations, in conjunction with our findings on the centrality of SRC-3 in EPC and transcription activation, raised the possibility that gene body SRC-3 binding sites could be involved in transcriptional regulation due to looping interactions with enhancers and/or promoters.

Therefore, we treated MCF-7 cells E2 and performed 3C-qPCR to map the contacts of the *GREB1* enhancer and promoter with two prominent internal gene body SRC-3 binding sites GBS1 and GBS2, at 18 kb and 43 kb downstream of the *GREB1c* TSS, respectively (Figure S1L). Contact efficiencies (Looping Index^{3C}) in E2-treated cells (60′) were normalized to the untreated (0′) and were presented as Fold-change in Looping Index^{3C} (Figure 4A). We detected contacts of the enhancer and promoter with both GBS1 and GBS2; E2 strongly enhanced the Enh-preTSS, Enh-postTSS, preTSS-GBS1 and postTSS-GBS1 contacts. Interestingly, Enh-GBS1, Enh-GBS2, preTSS-GBS2 and postTSS-GBS2 contacts also were detected in hormone-deprived cells (0′), of which Enh-GBS2 and postTSS-GBS2 diminished over E2 treatment.

Several of these contacts were recapitulated in the IV3C assay, where we used the *GREB1* BAC clone CTD-2563K11 as the template DNA (Figure 4B). Continuing from the Enh-preTSS and Enh-postTSS contacts described in Figure 2F, we observed strong ERα-dependent Enh-GBS1, preTSS-GBS1, postTSS-GBS1, preTSS-GBS2 and postTSS-GBS2 contacts. While the Enh-GBS2 contact seemed enhanced by ATP, the PostTSS-GBS1, Enh-GBS2, PreTSS-GBS2 and PostTSS-GBS2 contacts diminished in conditions that simulated active transcription. Figure S4A provides a comparative assessment of fold change in contacts upon E2 induction in MCF-7 cells (3C) and upon transcription in vitro on CTD-2563K11 (IV3C).

GBS1 and GBS2 stimulate transcription in vitro—The above results raised the possibility that GBS1 and GBS2 might interact with the enhancer and promoter fragments in

Author Manuscript Author Manuscript Author Manuscript Author Manuscript

vitro. Expectedly, we observed strong retention of both GBS1 and GBS2 with both Biot.F1 and Biot.F6 in *trans*-Interaction assays (Figure 5A). GBS1 retention with Biot.F6 was almost 10-fold higher compared to with Biot.F1, suggesting its preferential contact with the promoter. On the other hand, GBS2 showed 4-fold higher interaction with the enhancer compared to the promoter. These observations suggested that GBS1 and GBS2 might impact transcriptional output from the enhancer and the promoter. Interestingly, both GBS1 and GBS2, but not F3, individually stimulate eRNA and mRNA production from CompF in vitro, and more so when present together (Figure 5B), suggesting that the interactions of GBS1 and GBS2 with the enhancer and promoter have transcriptional relevance. GBS2 also stimulates transcription from the BAC clone CTD-3138J7, which lacks the GBS2 region (Figure S4B). Surprisingly, GBS2 can stimulate mRNA production from CompFΔF1 in the absence of the enhancer (Figure S4C). In sum, the above data reveal that both enhancer and promoter make contacts with gene-body SRC-3 binding sites both in cells and in vitro, and that such contacts likely have regulatory roles in transcription.

Dynamic chromatin interaction landscape at the *GREB1* locus

To understand the relevance of such contacts further, we carried out E2-treatment time-course analyses in MCF-7 cells using 3C-qPCR assays; nascent transcript synthesis along the *GREB1* gene was quantified at exactly the same time points (Figure 6A). Fold change in the magnitudes of contacts for each pair of interacting loci at each time point are shown in Figure S5 (also see Figure 6D). These values for each interacting pair at each time point were employed in manually creating the connectivity diagrams for each time point (Figure 6B; the connectivity schematic is shown above). In Figure 6B, each interrogated site is depicted as a color-coded circle. Juxtaposition and the extent of overlaps between two circles reflect the magnitude of contact, whereas no contacts were observed between sites whose representative circles do not touch each other. For example, strong contacts between the enhancer and GBS2 in E2-deprived cells (no E2) is depicted by overlapping E and G2 circles, whereas these circles stand apart at 5 min post E2, reflecting their disengagement upon E2 stimulation. Below each connectivity map the nascent transcript levels at the enhancer (Enh), PostTSS (Pro), GBS1 and GBS2 quantified at the indicated time point are shown (Figure 6C). We compared the magnitudes of chromatin interactions for each pair to that of the underlying transcription at the same sites, in order to understand the transcriptional relevance of the connections.

These connectivity maps reveal that: (1) the enhancer remains in strong, direct contact with GBS1 and GBS2 in unstimulated cells, while the promoter is held in the vicinity of the enhancer by virtue of its contacts with GBS1 and GBS2. (2) E2 stimulation induces swift changes in these connections: GBS1 and GBS2 promptly disengage from the enhancer, which now contacts both preTSS and postTSS sites directly. (3) GBS1 comes back in contact with the enhancer within 10 minutes, and this corresponds to a noticeable increase in transcription detected at GBS1. (4) GBS2 stays away from the enhancer until 60 minutes post-E2 treatment, when GBS2 is evidently undergoing transcription; preTSS-GBS2 follows kinetics similar to that for Enh-GBS2. (5) PostTSS-GBS1 contact is formed immediately after E2 stimulation, but it weakens over time before becoming stronger again at 60 minutes

Author Manuscript Author Manuscript Author Manuscript Author Manuscript

(Figure S5; Figures 6B, 6D). Note that the contact efficiency for the control pair Enh-F2 remains largely unaltered.

These observations suggest that after E2 stimulation, actively transcribing regions stay in direct contact with the enhancer, and newer regions make contacts with the enhancer as they undergo active transcription (e.g., Enh-GBS1 contact is reestablished within 10 min, and Enh-GBS2 contact within 60 min). Also noteworthy is the sharp GBS1-GBS2 contact at 5′ after E2 stimulation, which quickly diminishes, and the swift disengagement of the preTSS-postTSS ends of the promoter upon E2 induction (Figure S5; Figure 6D).

The findings that the *GREB1* enhancer and promoter are held in close proximity in unstimulated cells, and rapidly contact each other upon stimulation, mirror the mutual transcriptional stimulation of the enhancer and promoter as seen in our in vitro looping assays. We also examined the chromatin interaction landscape at the *NRIP1* locus (Figure S6A; see the connectivity maps in Figure S6B). We observed that the dynamics between the contact pairs are surprisingly very similar to *GREB1* (compare Figure S6B to Figure 6B), suggesting a greater generality of dynamism in chromatin interaction landscape.

In summary, the above data present an unprecedented view of the dynamic looping interactions that occur during E2-induced transcription of an ERα target gene.

SRC-3 is required for maintaining dynamic chromatin interactions at ERα-target genes

Given the centrality of SRC-3 in EPC (Figure 3), we conducted time-course chromatin connectivity mapping in MCF-7 cells transfected with siRNAs targeting SRC-3 for 72 hours prior to E2 treatment. Interestingly, the chromatin interaction landscape almost was abolished upon SRC-3 knockdown (Figure 6D). Our observations suggest a strong role for SRC-3 in governing chromatin topology at the *GREB1* locus. Importantly, we observed a very similar effect of SRC-3 knockdown on chromatin interactions at the *NRIP1* locus (compare Figure S6C to Figure 6D).

Contact disengagements are important during transcription

The above results demonstrate that several contacts are disrupted during E2/ERα-mediated transcription activation. For instance, abrupt disengagement of GBS1 and GBS2 from the enhancer coincides with prompt establishment of the promoter's connection with the enhancer. Particularly, two connections stand out that either fail to disengage (e.g., preTSS-postTSS) or disengage with a much slower kinetics (e.g., preTSS-GBS2) in the absence of SRC-3 (Figure 6D). We reason that both dynamic establishment and severance of contacts in the chromatin topology might be crucial to the activation and processivity of transcription. Thus, we hypothesized that RNA Pol II transcription inhibition might "freeze" the connections, and impair the dynamics of connectivity.

To test this possibility, we employed inhibitors of RNA Pol II transcription and conducted both 3C and IV3C assays. For 3C assay, MCF-7 cells were pre-treated with 1 μM of the TFIIH initiation factor inhibitor triptolide (TRP; (Titov et al., 2011)) or the elongation factor P-TEFb inhibitor flavopiridol (FLV; (Chao and Price, 2001)) for one hour and then were further treated with 100 nM E2 for one hour. We mapped the connections and compared the

Author Manuscript Author Manuscript Author Manuscript Author Manuscript

magnitudes of E2-induced loopings to those after pretreatment with the two inhibitors. Figure 7A reveals that several connections are either stabilized or reduced in the presence of the inhibitors. For instance, the Enh-preTSS connection diminished in the presence of TRP, whereas Enh-PostTSS, Enh-GBS2, preTSS-GBS2, postTSS-GBS1, postTSS-GBS2, GBS1-GBS2 and preTSS-postTSS connections are stabilized with both inhibitor pre-treatments. PreTSS-GBS2 was 'kinetically' stabilized upon SRC-3 depletion (Figure 6D). Interestingly, FLV stabilized almost all of the interactions—preTSS-GBS1 and Enh-PreTSS being the only connections unaffected. The contacts stabilized by FLV correlate with those impaired by SRC-3 depletion (Figure 6D). With 1 μM pre-treatment, both these inhibitors completely abolished E2-induced *GREB1* transcription (Figure S7A).

We interrogated the effects of TRP and FLV on looping using our IV3C assay, where the inhibitors were added to the template DNA and reaction buffer before the addition of HeLa NE. Here again, preTSS-GBS1 remained largely unaffected, while FLV stabilized the other interactions (Figure 7B) — consistent with the observations in MCF-7 cells. Pre-treatment with the inhibitors abolished ERα-mediated activated transcription of mRNA and eRNA produced from the *GREB1* BAC clone in IVT reactions that are identical to the IV3C assays (Figure S7B).

Collectively, these results suggest that inter-region chromatin interactions within a gene locus correspond to specific transcription events, and when RNA Pol II transcription is inhibited, the dynamic interplay of these contacts is perturbed.

DISCUSSION

Cell-free assays for enhancer-promoter contacts (EPCs) and consequent transcription induction

In this study, we developed three new cell-free assays (Looping, *trans*-Interaction, and IV3C) to detect EPC occuring within an E2-stimulated, ERα target gene *GREB1* in the presence of HeLa S3 NE. Each assay revealed that the factors present in the NE alone have a baseline potential to promote EPC, which reflects pre-formed EPC at genomic loci (Ghavi-Helm et al., 2014; Jin et al., 2013; Phanstiel et al., 2017). Addition of ERα to the reactions enhances EPC, which is increased even further when active transcription ensues; this mirrors *de novo* EPC. Our experimental platform is the first to assay enhancer-dependent activation of promoter transcription (mRNA) and concurrent generation of eRNA in vitro. We showed that maximal EPC occurs when both the enhancer and promoter are undergoing active transcription. We further showed that isolated fragments of the enhancer and promoter not only interact in *trans*, but they also mutually stimulate transcription from each other. Our data suggest that the 'act of transcription' at the interacting pair of enhancer and promoter, but not their transcripts *per se*, is the basis of such mutual transcriptional stimulation. Further studies are required to define further the molecular mechanism of this mutualism. Our observation of the interacting enhancer and promoter transcribing coordinatively in vitro provides the first direct explanation for why 'active' enhancers (enhancers 'looping' to active promoters) always generate eRNAs in cells (Li et al., 2016). Importantly, these assays allow us to investigate questions about EPC that formerly could not be addressed in living cells. For example, by controlling the availability of ERα and NTPs we can study EPC in

Author Manuscript Author Manuscript Author Manuscript Author Manuscript

the context of transcriptional activation. Our assays can potentially be employed to understand the biochemistry and proteomics of transcriptional sub-reactions in greater depth. Further, we demonstrate the versatility of our assays by also showing serum-dependency of EPC and transcription activation at the *FOS* locus in vitro.

Although 3C technology is primarily used to interrogate structural aspects of chromatin in cellular contexts (Denker and de Laat, 2016; Spurrell et al., 2016), we have modified this technique into a cell-free assay (IV3C) to study EPC dynamics in greater detail. By interrogating the preTSS and postTSS regions of the *GREB1* promoter in our 3C and IV3C assays, we have been able to provide additional mechanistic understanding of EPCs in the context of activated transcription. For example, the Enh-preTSS interaction builds up over time, pointing to an important role for the enhancer in PIC formation. In contrast, the Enh-postTSS contact declines during transcription activation, possibly reflecting the progressive passage of the elongating RNA Pol II. Additionally, the gradual decline in preTSS-postTSS interaction after E2 induction indicates that the promoter chromatin undergoes extensive sequential structural changes during transcription. This dynamism is also recapitulated in our in vitro assays.

SRC-3 governs the dynamic chromatin landscape via intronic SRC-3-bound sequences

We identified SRC-3 as a key looping determinant in vitro and validated its requirement for establishing E2-directed chromatin interactions in MCF-7 cells. While SRC-3 is known to be required for ERα-dependent transcription activation both in vitro and in MCF-7 cells (Acevedo et al., 2004; Foulds et al., 2013; Shang et al., 2000; Won Jeong et al., 2012; Yi et al., 2015) and ERα is required for E2-induced EPC within the *GREB1* locus (Fullwood et al., 2009), our results reveal new mechanistic aspects of how SRC-3 promotes looping. Namely, (1) SRC-3 mediates ERα activation via direct interaction (Yi et al., 2015), and we now show its absence impairs EPC even when ERα is present; (2) ‘basal’ EPC (in the absence of ERα) is impaired upon SRC-3 depletion, suggesting that other transcription factors may be responsible for SRC-3 recruitment and subsequent EPC in this state; (3) ERα can still partly rescue EPC loss after SRC-3 depletion in our cell-free assays, suggesting that ERα potentially can partner with looping factors other than SRC-3, and (4) ERα instigates rearrangements of inter-region interactions that are bound by SRC-3.

Our E2 treatment time-course 3C experiments provide a previously unrealized picture of the dynamic chromatin interaction landscape at two human genes (*GREB1* and *NRIP1)*. This approach also reveals a prominent consequence of SRC-3 depletion: the near-complete abolition of chromatin interactions along both the genes examined. Future work is needed to elucidate exactly how SRC-3 manages to orchestrate these chromatin changes. Further, our results suggest that both the enhancer and the promoter are held in close proximity via their contacts with intronic SRC-3 bound sequences GBS1 and GBS2 in unstimulated cells. GBS1 and GBS2 disengage from the enhancer upon E2 induction, allowing direct enhancer-promoter contacts to occur. We additionally show that (1) *GREB1 and NRIP1* GBS1 returns to its contact with the enhancer when ‘active’ transcription is detected at GBS1; and (2) *GREB1* GBS2 resumes contact with the enhancer within 60 minutes, coincident with active transcription at GBS2. Our observations suggest that downstream transcribing regions of the

Author Manuscript Author Manuscript Author Manuscript Author Manuscript

gene are recruited back into contact with the enhancer progressively during transcription. This strong coordination of transcription at the enhancer and promoter is recapitulated in our looping-coupled cell-free transcription reactions.

Genome-wide ChIA-PET and Hi-C experiments have defined promoter-gene body interactions (Jin et al., 2013; Li et al., 2012; Siersbaek et al., 2017). Our observations provide a mechanistic relevance of such contacts and are consistent with a recent report that the enhancer remains in constant contact with the promoter during transcription of a gene and also makes progressive contacts within the gene body (Lee et al., 2015). Similarly, progressive promoter—gene body contacts have been reported for three TNFα-induced long genes during transcription (Larkin et al., 2012). These studies and our findings collectively suggest that the actual site of gene transcription remains in a relatively fixed nuclear 'bubble' that encompasses the enhancer, the promoter, and select downstream transcribing regions of the DNA that are progressively pulled into this bubble as transcription continues. We propose that preformed contacts of the promoter and enhancer with select gene-body locations (e.g., GBS1 and GBS2 for *GREB1*) are necessary for keeping an entire DNA transcription unit in the neighborhood of the bubble so that enhancer and promoter transcription can occur there in a coordinated fashion without the need for longitudinal transgression of the polymerase complex along the vast length of a gene. In other words, the DNA sequences of a gene may be looped back to the transcriptional bubble containing the transcription machinery. Additionally, our data suggests that gene-body sequences have a role in stimulating enhancer and promoter transcription in vitro. Additional future investigation will be required to fully validate the relevance of GBS1, GBS2 and other internal gene-body squences in transcriptional activation of *GREB1* and other genes.

Importance of chromatin contact severance—Besides EPC, SRC-3 depletion also abolishes the preTSS-GBS2 and preTSS-post-TSS interactions. Since SRC-3 depletion abrogates transcriptional activation, this observation suggests the importance of contact disengagement and remodeling during transcription. Indeed, preventing transcription activation by pretreating MCF-7 cells (or addition to the cell-free assays) with RNA Pol II transcription inhibitors triptolide and flavopiridol yeilded results consistent with this model. Surprisingly, the majority of connections were still efficiently made in the presence of transcription inhibitors, yet they failed to disengage, emphasizing that both formation and severance of contacts are needed for transcription activation. Interestingly, previous studies have shown that EPC is maintained when induced transcription is blocked by transcription inhibitors (Palstra et al., 2008). Each cycle of contact formation and severance may reflect a dynamic cycle of re-initiation. Our cell-free assays can directly test this notion in the future by preventing re-initiation by simple addition of Sarkosyl to the 'transcription' (Hawley and Roeder, 1985).

In summary, using our new looping assays, we have interrogated the dynamics of interactions among an enhancer, promoter and select gene-body sequences in the context of ERα-dependent transcription of the human *GREB1* gene, detailing an intricate cycle of chromatin interactions that correspond temporally and functionally with transcription. We further found that SRC-3 has a crucial role in modulating these dynamic changes. Our

Author Manuscript Author Manuscript Author Manuscript Author Manuscript

methodologies serve as a powerful platform to address many future questions in enhancer function.

STAR METHODS

KEY RESOURCES TABLE

REAGENT or RESOURCE	SOURCE	IDENTIFIER
Antibodies		
SMC1	Bethyl Laboratories	A300-055A
SMC3	Bethyl Laboratories	A300-060A
RAD21	Bethyl Laboratories	ab154769
MED12	Bethyl Laboratories	A300-774A
CDK8	Bethyl Laboratories	A302-500A
HDAC1	Bethyl Laboratories	A300-713A
SRC-1	Santa Cruz Biotechnology	1135/H4; sc-32789
SRC-2	BD Biosciences	610985
SRC-3	Custom mouse mAb generated at Baylor College of Medicine	N/A
RNA Pol II (RPB1)	Active Motif	101307
ERα	Santa Cruz Biotechnology	HC-20; sc-543
YY1	Bethyl Laboratories	A302-779A
Mouse IgG	Santa Cruz Biotechnology	sc-2025
Rabbit IgG	Santa Cruz Biotechnology	sc-2027
ECL Anti-Rabbit IgG-HRP conjugate	GE Healthcare UK	NA934V
ECL Anti-Mouse IgG-HRP conjugate	GE Healthcare UK	NA931V
Chemicals, Peptides, and Recombinant Proteins		
TRI-Reagent	Molecular Research Center	TR-118
BAN (4-bromoanisole)	Molecular Research Center	BN-191
Triptolide	Sigma-Aldrich	T3652
Flavopiridol	Sigma-Aldrich	F3055
Poly(vinyl alcohol)	Sigma-Aldrich	P8136
Q5 High-Fidelity DNA Polymerase	New England Biolabs	M0491
OneTaq Hot Start DNA Polymerase	New England Biolabs	M0481L
PstI	New England Biolabs	R0140L
Recombinant estrogen receptor alpha (ERα)	Thermo Fisher Scientific	A15674
T4 DNA Ligase	New England Biolabs	M0202S
17-β Estradiol (E2) (water-soluble)	Sigma-Aldrich	E4389
Glycogen	Sigma-Aldrich	G1767
Critical Commercial Assays		
TURBO DNA-free kit	Invitrogen/Ambion	AM1907
SensiFAST SYBR Hi-ROX One-Step kit	Bioline	BIO-73005

Author Manuscript Author Manuscript Author Manuscript Author Manuscript

REAGENT or RESOURCE	SOURCE	IDENTIFIER
SYBR Green PCR Master Mix	Applied Biosystems	4309155
Gibson Assembly Cloning Kit	New England Biolabs	E5510S
TOPO TA Cloning Kit	Invitrogen	K450001
Lipofectamine RNAiMax	Invitrogen	13778150
ECL Plus Western Blotting Substrate	Pierce	32132
Experimental Models: Cell Lines		
MCF-7	Tissue Culture Core, Baylor College of Medicine	N/A
HeLa	Tissue Culture Core, Baylor College of Medicine	N/A
HeLa S3 (for making bulk NE)	Cell Culture Company, LLC	HA48
Oligonucleotides		
Please see Supplemental Table S1		
Recombinant DNA:		
GREB1 BAC clone CTD-3138J7	Invitrogen	CTD-3138J7
GREB1 BAC clone CTD-2563K11	Invitrogen	CTD-2563K11
NRIP1 BAC clone RP11-1025G18	Invitrogen	RP11-1025G18
FOS BAC clone CTD-2655F5	Invitrogen	CTD-2655F5
pIE-0	(Pazin et al., 1994)	NA
Other		
M280 Streptavidin Dynabeads™	Invitrogen	60210
Protein A Agarose	Invitrogen	15918-014
Protein G Sepharose 4B	Invitrogen	101242
Quantum Prep PCR Kleen Spin Columns	Bio-Rad	732-6300

CONTACT FOR REAGENT AND RESOURCE SHARING

As Lead Contact, Bert W. O'Malley is responsible for all reagent and resource requests. Please contact Bert W. O'Malley at berto@bcm.edu with requests and inquiries.

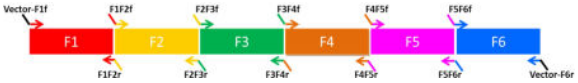
METHOD DETAILS

Constructs and templates for looping and IVT assays—Six regulatory regions of the *GREB1* locus, referred to as F1 through F6 (1.1-1.3 kb each), were amplified from either MCF-7 genomic DNA or the BAC clone CTD-3138J7, using high-fidelity Q5 DNA polymerase (NEB). F1 was subcloned into pIE0 (Pazin et al., 1994) by conventional cloning; fragments F2, F3, F4, F6 were subcloned into pCR2.1 by Topo-cloning (Invitrogen); F5 was cloned into pCR4 (Foulds et al., 2013). The clones were sequenced to verify correctness. The six fragments were PCR-amplified and assembled into a composite construct called "CompF" by Gibson assembly kit (following the manufacturer's protocol) into pCR2.1 (see below). GBS1 and GBS2 were amplified from MCF-7 genomic DNA using Q5 DNA polymerase. Where required, the individual fragments or the CompF were amplified in bulk using unmodified or 5′-biotinylated primers and OneTaq DNA polymerase (NEB), with the plasmid subclones (for F1-F6, or CompF) or Q5 PCR products (for GBS1 or GBS2) as template DNA. Primers were obtained from either Sigma-Aldrich (The Woodlands, TX) or

Author Manuscript Author Manuscript Author Manuscript Author Manuscript

Integrated DNA Technologies (IDT). All PCR products were purified over PCR Kleen columns (Bio-Rad) before use.

Generation of CompF by Gibson assembly—Fragments F1 through F6 were amplified with primers that overlapped the pCR2.1 vector (for F1 and F6) or among themselves (F1-F2, F2-F3, F3-F4, F4-F5, F5-F6) as shown in the schematic below:



Unique restriction enzyme sites were incorporated at inter-fragment junctions (see the color-coded oligonucleotides listed above) as follows:

Restriction sequence at the junctions (see oligonucleotide sequences below):

Before F1	ggatcc	*Bam*HI
F1F2f, F1F2r (F1-F2)	gacgtc	AatII, *Zra*I
F2F3f, F2F3r (F2-F3)	gtcgac	*Sal*I
F3F4f, F3F4r (F3-F4)	cccggg	*Xma*I, *Sma*I
F4F5f, F4F5r (F4-F5)	atcgat	*Cla*I
F5F6f, F5F6r (F5-F6)	ccgcgg	*Sac*II
After F6	gaattc	*Eco*RI

All fragments were amplified from their respective plasmids using the primer pairs shown above using Q5 high-fidelity DNA polymerase. Vector pCR2.1 was linearized with *Eco*RI. All fragments and the linear vector were gel-purified using the Qiagen gel-extraction kit. Gibson assembly was carried out with 0.2 pmoles of each DNA species and 2x Gibson Assembly Master Mix in total volume of 20 μl. The final product (2 μl) was transformed into Top10 beta competent *E.coli* cells. Colonies were screened by digesting the plasmids with *Hin*dIII. Positive clones from the screen were Sanger sequenced for verification.

Experimental Model—MCF-7 cells (ATCC; from Baylor College of Medicine Tissue Culture Core) were grown in DMEM without phenol red, supplemented with 5% charcoal-stripped fetal calf serum (csFCS). Cells were transfected with 25 nM Mission siRNA Universal Negative Control #1 duplexes (siNT; Sigma-Aldrich) or 25 nM siRNA duplexes targeting SRC-3 using Lipofectamine RNAiMax transfection reagent. Cells were harvested for lysate preparation and RNA extraction (Figures S3F and G; 6-well plates) or for 3C (Figure 3E; 10 cm plates) 72 hr post-transfection. Where required, cells were treated with 100 nM E2 (Sigma) for the designated time period prior to harvesting (Figure 6A). For nuclear extract (NE) preparation, cells were grown in regular DMEM with 10% FCS in 15 cm plates. To prepare NE from serum-starved and serum-stimulated HeLa cells, 12×15cm plates were used where cells were grown to about 90% confluence. All plates were then grown in serum-free DMEM for 48 hr. Fresh DMEM was added to six plates (Starved), while the remaining six received fresh DMEM+10%FBS for 2 hr (+FBS). NE was prepared

Author Manuscript Author Manuscript Author Manuscript Author Manuscript

from both cells as described below, and were used for experiments in Figures 1F and S2H. For 3C experiments (Figure S2D) HeLa cells were grown to about 80% confluence in 10cm plates and serum-starvation and stimulation were conducted exactly as described above. Cells were x-linked with 1% formaldehyde after 2 hr serum stimulation (or fresh DMEM for "Starved") and processed for 3C as described below.

Nuclear extract (NE) preparation—NE preparations from HeLa S3 and MCF-7 cells were performed as described (Foulds et al., 2013). HeLa S3 NE preparation was adapted from (Dignam et al., 1983). Briefly, pellet from 20L of HeLa S3 cells (from National Cell Culture Center) was swollen in two packed cell volumes (pcv) of Buffer A and lysed using a B type Dounce homogenizer. Nuclei were collected by centrifugation (5000 rpm, 10 min, 4°C), and lysed in one pcv of Buffer C by further Dounce homogenization. The soluble fraction was collected after centrifugation (20000 × g; 20 min, 4°C) and dialyzed against 2L of Buffer D. Protein concentration was determined by Bradford assay (Bio-Rad), and conductivity were monitored on a conductivity meter with a KCl standard curve. NEs were snap-frozen in liquid N2 and stored at −80°C until use. MCF-7 NE preparation was performed as described (Lanz et al., 2010).

Basal looping and IVT assay conditions

Reaction conditions: The basal conditions for all the looping assays (looping assay, *trans*-Interaction assay, IV3C) and IVT were identical. A typical reaction (50 μl) contained 0.2 pmoles of DNA template (CompF, each individual fragment when in combination, or the BAC clones) in 12 mM Hepes-KOH (pH 7.9), 12% glycerol, 60 mM KCl, 12 mM $MgCl_2$, 0.12 mM EDTA, 0.3 mM DTT, 1 mM ATP, 0.9 mM acetyl CoA, 2% Poly(vinyl alcohol) prepared with DEPC-treated H2O as a 10% stock, 100 nM E2, and 50 μg NE. Reactions were incubated at room temperature (RT) for 25 min. Where required, 0.5 mM NTPs (an equimolar mixture of GTP, TTP and CTP) were added to the reactions, and shifted to 30°C for 45 min to allow transcription to progress (the 'transcription condition'). Where required, 1.8 pmoles of ERα (Invitrogen) was used in reactions with CompF or the BAC clone; whereas 0.9 pmole of ERα was used in reactions containing individual fragments (due to differences in template DNA size) [However, see note on ERα below]. For "no NE" controls, 50 μg BSA was used. For experiments in Figures 1F and S2D, 0.2 pmoles of the BAC clone CTD-2655F5 was used alongside 50 μg NE prepared from serum-starved or serum-stimulated HeLa cells. The reactions did not contain E2.

All HeLa S3 NE-based reactions had 100 nM E2. All reactions based on MCF-7 NE were essentially without E2, but 100 nM E2 was added where required.

Low-adhesion microcentrifuge tubes (e.g., BioExpress C-3302-1) were used in all assays without exception.

Replicates and qPCR: Every IVT and looping/*trans*-Interaction assay was always done in duplicate reactions. qPCR for each sample for each primer pairs was done in triplicates. Most data presented here represent 4-6 independent assay replicates (with three qPCR readings for each replicate).

Author Manuscript Author Manuscript Author Manuscript Author Manuscript

A note on ERα: We have observed wide differences in ERα specific activities from various lot #s (Invitrogen/ThermoFisher A15674). We typically assess the ERα quality using three different assays: (1) F1 or F6 DNA pulldown (as in Figure S1B) followed by immunoblotting to see ERα-dependent recruitment of SRC-3 and other co-regulators, (2) CompF IVT (naked or chromatinized) to see ERα-dependent transcription activation of eRNA or mRNA, and (3) a quick F1-F6 *trans*-Interaction assay. The actual amount of ERα required per assay is determined based on these initial assays, while keeping the NE amount constant. An excess ERα can inhibit looping and transcription by a squelching effect.

Looping assay—0.2 pmole of 5′Biot.CompF and DBiot.CompF were immobilized on 15 µl M280 streptavidin-coated Dynabeads™ and incubated with 50 µg NE with or without 1.8 pmole of ERα as above. The nucleoprotein complexes were cross-linked with 0.5% formaldehyde (Sigma) for 5 minutes at RT, quenched with 0.125M glycine (Sigma), pulled down using a magnetic platform, and washed twice with 200 µl Buffer D, once with 200 µl NETN, and once with 100 µl CutSmart buffer (NEB). The beads were resuspended in 50 µl CutSmart buffer containing 2 µl of *Sac*II, and digested at 37°C for 2 hr. One µl of this suspension was added to 50 µl of H_2O as the "Input (Inp)". The beads were pulled-down and the unbound fractions were collected; one µl was saved in 50 µl H_2O as the "*Sac*II-released (R)" fraction. The residual beads were washed 1 × 200 µl Buffer D, resuspended in 50 µl H_2O, and 1 µl of the suspension was saved in 50 µl of H_2O as the "Bound (B)" fraction. One µl of these three samples were diluted to 200 µl with H_2O, and 2 µl of the diluted samples were added to qPCR reactions to quantitate F1. *Sac*II cleavage efficiency is always monitored as shown in Figure S1C. Chromatinized CompF is not adequately cut by *Sac*II, rendering CompF chromatin unsuitable for the looping assay.

The following quantification pipeline was used to calculate the "Looping Index":

Calculation for both F1 and F6, and for both DBiot and 5′Biot.CompF							Calculation for both DBiot and 5′Biot.CompF	Looping Index
CT_R	**CT_B**	**CT_{Inp}**	**Calculate ΔCT_R and ΔCT_B**	**Calculate Released (R)**	**Calculate Bound (B)**	**Fraction Bound after SacII (fB)**	**F6 Enrichment over F1 ($F6_{eF1}$)**	
CT values for both F6 and F1 qPCR; from both 5′Biot and DBiot experiments			$\Delta CT_R = CT_R - CT_{Inp}$ $\Delta CT_B = CT_B - CT_{Inp}$	R=power(2, $-\Delta CT_R$)	B=power(2, $-\Delta CT_B$)	=B/(R+B)	=fB_{F6}/fB_{F1}	=(5′Biot_$F6_{eF1}$)/(DBiot_

*Sac*II cleavage efficiency is always monitored as shown in Figure S1C. We typically achieved >80% cleavage and equally for both 5′Biot and DBiot CompF. Chromatinized CompF is not adequately cut by *Sac*II, rendering CompF chromatin unsuitable for the looping assay.

Instead of F1, primers specific for F2 were used alongside F6 primers in calculating the Looping Index shown in Figure 2B.

Author Manuscript Author Manuscript Author Manuscript Author Manuscript

***trans*-Interaction assay—**0.2 pmole of Biot.F1 were immobilized on 10 μl M280 Dynabeads™ and F6, HeLa S3 NE, and ERα were added to final 50 μl as described above (see basal assay conditions) to examine F6 enrichment on F1. Conversely, Biot.F6 was immobilized and F1 was added to it alongside the NE and ERα to examine F1 enrichment on F6. *Alternatively*, biotinylated and unbiotinylated fragments were mixed with 50 μg HeLa S3 NE and ERα in solution and incubated for desired time points. Ten μl of M280 Dynabeads, washed with Buffer D, were added to each reaction to pulldown the nucleoprotein complexes. Both approaches, i.e. binding the biotinylated fragments to M280 beads first and then assembling the complexes, or assembling the reactions in solution first and then pulling down the biotinylated fragments gave similar results. The bound materials were washed twice with 200 μl Buffer D (+0.1% Igepal), once with 200 μl NETN, and resuspended in 50 μl 2x SDS sample buffer (with 2-mercaptoethanol). The samples were incubated at 80°C for 30 min to release the bound DNA fragments. One μl of the supernatant (released DNA) was serially diluted with H_2O 1:100 twice. Five μl of the diluted samples were quantitated by qPCR using primer pairs specific for F1 and F6. The ratio of unbiotinylated fragment enrichment ("prey") to biotinylated fragment ("bait") represents the *"trans*-Interaction Index".

Combination pulldown: Combination pulldown (Figure 3H) was essentially similar to *trans*-Interaction assay, except that 1.5 pmoles of F6 and Biot.F1 were used along with 250 μg NE, with or without 5 pmoles of ERα. Pulled down protein-DNAs were resuspended and denatured in 40 μl 2X SDS sample buffer; 10 μl of the samples were analyzed by immunoblotting alongside 3% of input NE run in parallel.

In vitro 3C (IV3C) assay—0.2 pmole of the BAC clone (CTD-3138J7 and CTD-2563K11 for *GREB1*, RP11-1025G18 for *NRIP1*, or CTD-2655F5 for *FOS*, wherever mentioned) was incubated with 50 μg NE with or without 1.8 pmole ERα (for HeLa NE) and with or without 100nM E2 (MCF-7 NE; see "Basal looping and IVT assay conditions" above). The nucleoprotein complexes were crosslinked with 0.5% formaldehyde and quenched with 0.125M glycine. The nucleoprotein complexes were separated from formaldehyde, glycine, buffer components, and smaller soluble proteins over the Quantum-prep PCR Kleen spin columns (Bio-Rad) following the manufacturer's instructions. The eluted samples were diluted two-fold (to 100 μl) with H_2O and 10X NEB3.1 buffer to final a 1.1x concentration, and digested with 2 μl *Pst*I (NEB) overnight at 37°C. On the next day, SDS was added to final 0.5%, and the samples were incubated at 65°C for 20 min. Triton x-100 was then added to the samples to final 1%, which were then incubated at 37°C for 30 minutes. The samples were then diluted with 1 ml of 1.2x ligation buffer containing 40 U of T4 DNA ligase (total dilution of reaction samples: 20x). Ligation was carried out for 2 hr at 16 °C. De-crosslinking and de-proteinization was carried out by incubating the samples with 5 μl Proteinase K (100 μg) at 65 °C overnight. The DNA was extracted with phenol-chloroform, precipitated with ethanol in the presence of 20μg glycogen, and dissolved in 100 μl H_2O. One μl of this sample was used in the first-round of PCR for the ligants. PCR (20 μl reactions) included 0.2 mM primers, and was performed with OneTaq DNA polymerase (NEB) with the following cycling conditions: 30 sec denaturation at 94 °C, [15 sec 94 °C, 20 sec 62 °C, 60 sec 68 °C] × 20 cycles. One μl of the PCR product was next added to 20 μl

Author Manuscript Author Manuscript Author Manuscript Author Manuscript

qPCR mix containing 0.1 mM ‘Round 2’ “nested” primer pairs in SYBR-Green PCR Mix (Applied Biosystems). qPCR reactions were performed on a Step ONE Plus real-time PCR machine (Applied Biosystems). One ng of a previously cut-and-ligated BAC DNA was run for PCR and qPCR in parallel to the assay samples. IV3C was not possible on chromatin templates, since we were unable to reconstitute the BAC into chromatin.

In vitro transcription (IVT)—0.2 pmole of template (naked or chromatin derivatives of CompF, or BAC DNA as indicated) was incubated with 50 μg of HeLa S3 NE with or without ERα as described above (see note on ERα). After 25 min at RT for PIC assembly, 5 μl of 5 mM NTP mixture (GTP, CTP, TTP) was added to the reactions and shifted to 30 °C for 45 minutes. 250 ul of Tri-Reagent was added to each reaction and mixed by vortexing. Next, 15 μl of BAN (4-bromoanisole) was added, mixed by vortexing, and incubated on ice for 15 min. The samples were then centrifuged at 15,000 rpm in a table-top microcentrifuge for 15 min at 4°C. 170 μl of the clear aqueous phase was transferred to a fresh microfuge tube, 20 μg glycogen was added to each tube, mixed, and RNA was precipitated with 150 μl of isopropanol for 20 min at RT. RNA precipitates were collected at 15,000 rpm in a table-top microcentrifuge for 15 min at 4°C; washed with 75% ethanol (prepared with DEPC-treated H_2O; Ambion) at RT, air-dried, and dissolved in 35 μl DEPC-treated H_2O at 55°C for 10 min. The RNA samples were digested with 1 μl of DNase (Turbo DNA-free kit; Ambion) along with 4 μl of DNase buffer as recommended by the manufacturer. DNase digestion was carried out for 1 hr at 37°C, and the reactions were stopped by adding the DNase inactivation reagent. Two μl of the resultant RNA sample (5% from 40 ul; equivalent to 10 fmoles of the template) was used in each One-step RT-qPCR reaction using the F6 primer pair. To verify that no significant “carry-over” DNA contamination remained after DNase digestion, each sample was also subjected to parallel qPCR reactions without reverse transcriptase (see Figure S2E). The CT values were normalized to an amplicon from 10 fmoles of template DNA, which is equivalent to the template amount in the RNA sample if it were not destroyed by DNase treatment. For example, *GREB1* eRNA was quantified based on amplicon from 10 fmoles of F1 template DNA, whereas *GREB1* mRNA was quantified based on amplicon from 10 fmoles of F6 template DNA. The resultant values were expressed as “relative transcription”. Also, the transcript levels across the samples in an experiment were normalized to that in the HeLa S3 NE only (basal transcription; without ERα), and the values were expressed as “fold activation” (Figure 5B). Every IVT experiment was always done in duplicate reactions, with three RT-qPCR reactions on each replicate sample.

3C (Chromosome Conformation Capture)-qPCR—The basic 3C methodology was adapted from (Hagege et al., 2007). MCF-7 cells grown on 10 cm plates to roughly 90% confluency were treated with 100 nM E2 for desired time points, crosslinked with 1% formaldehyde and quenched with 0.125M glycine. Cells were rinsed twice with cold PBS, and scraped from the plates with 5 ml Cell Lysis Buffer (supplemented with 1x Complete Mini protease inhibitor cocktail, Roche), followed by three washes in cold Cell Lysis Buffer (3 × 1 ml) and two washes in 1.2x NEB3.1 buffer (2 × 0.2 ml). Cells were resuspended in 200 μl 1.2x NEB3.1, SDS was added to final 0.3%, and samples were incubated at 37 °C for 1 hr. Triton X-100 was added to final 1% and samples were incubated at 37 °C for 1 hr.

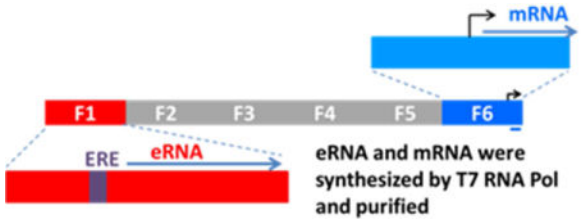
Author Manuscript Author Manuscript Author Manuscript Author Manuscript

Samples were then digested with 15 μl of *Pst*I (NEB; 300U total) at 37 °C overnight with gentle mixing. Next day, SDS was added to final 0.6%, and the samples were incubated at 65 °C for 30 min. Samples were diluted with 1.4 ml 1.15x T4 DNA Ligation Buffer (with 1% Triton X-100) and incubated at 37°C for 1 hr. DNA ends were then ligated with 100 U of T4 DNA Ligase for 4 hr at 16°C. The samples were de-proteinized and de-crosslinked by incubating at 65 °C overnight in presence of 10 μl (100 μg) Proteinase K. DNA was extracted with phenol-chloroform, precipitated with ethanol, and dissolved in 100 μl H_2O. Samples aliquoted before *Pst*I digestion, after digestion and after ligation were analyzed by PCR to monitor the digestion and ligation efficiencies. As in IV3C, the ligant detection quantitation of crosslinking efficiency involved two rounds of PCR: regular PCR in round 1, followed by qPCR in round 2. One μg of DNA was used per sample in the round 1 PCR. One μl of round 1 PCR product was used in each qPCR reaction.

Quantification and presentation of 3C/IV3C data: During each 3C/IV3C experiment, we digested BAC clone DNA with PstI, ligated, and purified the ligants. This "previously cut-and-ligated BAC DNA" served as a source for inter-fragment ligants that represent a theoretical optimum for ligant abundance. One ng of this "normalizer" ligant population was subjected to PCR and qPCR alongside the samples. We subtracted the "normalizer" C_T values for each primer pair from the corresponding C_T values obtained from the samples. This subtraction (ΔC_T) for each amplicon (each primer pair) was used the calculate the relative ligant abundance ($2^{\wedge -\Delta CT}$), which is same as contact efficiency. This value is presented here as "Looping Index". These BAC-normalized values were further normalized to the values in untreated (E2-deprived, or 0′) cells to obtain the "Fold change in Looping Index^{3C}" as presented in Figures 4A, 6D, 7A, and S5.

For *NRIP1* and *TFF1* 3C the sample ΔC_T values were calculated by subtracting the C_T value of 1% of the enhancer amplicon from each sample C_T values. The Fold change values for *NRIP1* 3C were calculated by normalizing the untreated (0′) sample ligant magnitudes to 1.

Synthesis of eRNA and mRNA—To supplement IVT/*trans*-Interaction with synthetic eRNA and mRNA as described in Figure 2H, portions of F1 and F6 corresponding to known eRNA and mRNA transcribed regions were amplified such that the new fragments contained T7 promoter sequence (see schematic below; see primer sequences above). The fragments were transcribed with T7 RNA polymerase (NEB) following manufacturer's recommendations. The reactions were digested with Turbo RNase-free DNase. RNA was precipitated following TRI-reagent extraction, dissolved in DEPC-treated H2O and quantified.



Author Manuscript Author Manuscript Author Manuscript Author Manuscript

One pmole eRNA/mRNA thus prepared was added to the reactions with 0.2 pmole F6/F1 (Figure 2H)

Immunodepletion—Immunodepletion of antigens from HeLa S3 NE was performed as described (Foulds et al., 2013) except that Buffer D was used instead of PBS. A mixture of protein A agarose and protein G agarose beads (50% slurry; 20 μl each per mg NE) was washed with Buffer D and pre-blocked with 1 mg/ml BSA (Sigma, fraction V) in Buffer D for 1 hr. Five μg of either control IgG (rabbit or mouse depending on the target antibody) or target antibody (Ab) were bound to the pre-blocked beads in final 150 μl Buffer D overnight. On the next day, the beads were washed once in Buffer D and 1 mg HeLa S3 NE was added. Two rounds of immunodepletion were carried out at 4°C for 2 hr each. The beads were gently pelleted by centrifugation (1500 rpm, 30 sec.) on a bench top microcentrifuge, and the supernatant was transferred to a fresh microfuge tube containing pre-blocked, IgG-bound beads for the second round. The final supernatant was saved as the immunodepleted NE. Protein concentration was monitored after immunodepletion by Bradford assay. For cohesin immunodepletion, antibodies to SMC-1 and SMC-3 were used together (5 μg each, per round, for 1 mg NE). Rabbit IgG was used as controls for immunodepletion of cohesin, MED1, MED12, CDK8, and HDAC1, whereas mouse IgG was used as control for immunodepletion of SRC-3.

Chromatin reconstitution: Eight μg of each fragment (F1, F6, CompF) was mixed with 12 μg HeLa core histones in the presence of 2M NaCl in 1x CRB (10 mM Tris-HCl (pH 7.5), 1mM EDTA, 0.05% Igepal) in final 15 μl, and let stand at room temperature (RT) for 20 minutes. Thereafter, the nucleohistone mixture was diluted by adding 1xCRB every 20 minutes in the following sequence: 5, 5, 5, 7.5, 12.5, 25 μl, and finally 75 μl (with 0.5mg/ml BSA, to final 0.25mg/ml). This led to gradual decrease in the NaCl concentration to 1.5, 1.2, 1, 0.8, 0.6, 0.4, and finally 0.2M, during which time the nucleohistone mixture assembles into chromatin. The chromatin thus prepared is stable for years at 4°C. The chromatin preparation was verified by limited micrococcal nuclease (MNase) digestion. 0.5 μg of chromatin was digested with 25U of MNase (Worthington) in final 2mM CaCl2 for 1 and 2 minutes at RT (Figure S1J). Digestion was stopped by adding EDTA to final 10 mM. The digests were deproteinized for a 15 minute digestion with Proteinase K followed by phenol-chloroform extraction and ethanol precipitation. The digests were run on a 2.5% agarose gel in 1xTG buffer at 4°C, stained with EtBr (Figure S1J). 0.2 pmoles of the chromatin templates were employed in *trans*-interaction assay (Figure S1I) or IVT (Figure S2E).

Immunoblotting—For immunodepleted NE and siRNA-transfected whole cell extracts, 50 μg proteins were resolved on SDS-PAGE (4-15% acrylamide gradient), transferred onto PVDF membrane (Bio-Rad), and immunoblotted following standard protocols (Foulds et al., 2013). HRP-conjugated secondary antibodies (anti-Rabbit and anti-Mouse) and ECL Plus reagents were used for immunoblot detection with X-ray film.

Data analysis—Quantitative PCR data were analyzed and plotted with MS Excel. T-test values were calculated with MS Excel. Immunoblot densitometric quantification was done with Image J.

Author Manuscript Author Manuscript Author Manuscript Author Manuscript

List of Buffers used—Buffer A: 10 mM HEPES (pH 7.9), 1.5 mM $MgCl_2$, 10 mM KCl; 0.5 mM DTT and 0.5 mM PMSF added before use.

Buffer C: 20 mM HEPES (pH 7.9), 25% glycerol, 0.42 M NaCl, 0.2 mM EDTA, 1.5 mM $MgCl_2$; 0.5 mM DTT and 0.5 mM PMSF added before use.

Buffer D: 20 mM Hepes-KOH (pH 7.9), 20% glycerol, 0.2 mM EDTA, 100 mM KCl; volume made up with DEPC-treated nuclease-free H2O (Ambion).

Cell Lysis Buffer (3C): 10 mM Tris-HCl (pH 7.5), 10 mM NaCl, 0.2% Igepal CA-630; supplemented with 1x protease inhibitor cocktail (Roche) and 0.2mM PMSF.

NETN: 20 mM Tris-KCl (pH 7.5), 150 mM NaCl, 1 mM EDTA, 0.5% Igepal CA-630

1x T4 DNA Ligase Buffer: 66 mM Tris-HCl (pH 7.5), 5 mM $MgCl_2$, 5 mM DTT, 1 mM ATP

Supplementary Material

Refer to Web version on PubMed Central for supplementary material.

Acknowledgments

This study was supported by NIH grants HD007875 and HD08818 and DoD grant W81XWH-13-1-0285 to B.W.O. We thank the following at BCM: Judy Roscoe and the Tissue Culture Core (for maintenance of MCF-7 cells), the Monoclonal Antibody/Recombinant Protein Shared Resource funded by NCI Cancer Center Support Grant 5 P30 CA125123 (for monoclonal SRC-3 in-house antibody), and the Gene Vector Core for providing Sanger sequencing of plasmid subclones.

References

Acevedo ML, Lee KC, Stender JD, Katzenellenbogen BS, Kraus WL. Selective recognition of distinct classes of coactivators by a ligand-inducible activation domain. Mol Cell. 2004; 13:725–738. [PubMed: 15023342]

Andrey G, Montavon T, Mascrez B, Gonzalez F, Noordermeer D, Leleu M, Trono D, Spitz F, Duboule D. A switch between topological domains underlies HoxD genes collinearity in mouse limbs. Science. 2013; 340:1234167. [PubMed: 23744951]

Banerji J, Rusconi S, Schaffner W. Expression of a beta-globin gene is enhanced by remote SV40 DNA sequences. Cell. 1981; 27:299–308. [PubMed: 6277502]

Blackwood EM, Kadonaga JT. Going the distance: a current view of enhancer action. Science. 1998; 281:60–63. [PubMed: 9679020]

Chao SH, Price DH. Flavopiridol inactivates P-TEFb and blocks most RNA polymerase II transcription in vivo. J Biol Chem. 2001; 276:31793–31799. [PubMed: 11431468]

Chen Y, Bates DL, Dey R, Chen PH, Machado AC, Laird-Offringa IA, Rohs R, Chen L. DNA binding by GATA transcription factor suggests mechanisms of DNA looping and long-range gene regulation. Cell Rep. 2012; 2:1197–1206. [PubMed: 23142663]

Deng W, Lee J, Wang H, Miller J, Reik A, Gregory PD, Dean A, Blobel GA. Controlling long-range genomic interactions at a native locus by targeted tethering of a looping factor. Cell. 2012; 149:1233–1244. [PubMed: 22682246]

Denker A, de Laat W. The second decade of 3C technologies: detailed insights into nuclear organization. Genes Dev. 2016; 30:1357–1382. [PubMed: 27340173]

Author Manuscript Author Manuscript Author Manuscript Author Manuscript

Dignam JD, Lebovitz RM, Roeder RG. Accurate transcription initiation by RNA polymerase II in a soluble extract from isolated mammalian nuclei. Nucleic Acids Res. 1983; 11:1475–1489. [PubMed: 6828386]

Euskirchen GM, Auerbach RK, Davidov E, Gianoulis TA, Zhong G, Rozowsky J, Bhardwaj N, Gerstein MB, Snyder M. Diverse roles and interactions of the SWI/SNF chromatin remodeling complex revealed using global approaches. PLoS Genet. 2011; 7:e1002008. [PubMed: 21408204]

Foulds CE, Feng Q, Ding C, Bailey S, Hunsaker TL, Malovannaya A, Hamilton RA, Gates LA, Zhang Z, Li C, et al. Proteomic analysis of coregulators bound to ERalpha on DNA and nucleosomes reveals coregulator dynamics. Mol Cell. 2013; 51:185–199. [PubMed: 23850489]

Fullwood MJ, Liu MH, Pan YF, Liu J, Xu H, Mohamed YB, Orlov YL, Velkov S, Ho A, Mei PH, et al. An oestrogen-receptor-alpha-bound human chromatin interactome. Nature. 2009; 462:58–64. [PubMed: 19890323]

Ghavi-Helm Y, Klein FA, Pakozdi T, Ciglar L, Noordermeer D, Huber W, Furlong EE. Enhancer loops appear stable during development and are associated with paused polymerase. Nature. 2014; 512:96–100. [PubMed: 25043061]

Hadjur S, Williams LM, Ryan NK, Cobb BS, Sexton T, Fraser P, Fisher AG, Merkenschlager M. Cohesins form chromosomal cis-interactions at the developmentally regulated IFNG locus. Nature. 2009; 460:410–413. [PubMed: 19458616]

Hagege H, Klous P, Braem C, Splinter E, Dekker J, Cathala G, de Laat W, Forne T. Quantitative analysis of chromosome conformation capture assays (3C-qPCR). Nat Protoc. 2007; 2:1722–1733. [PubMed: 17641637]

Hah N, Murakami S, Nagari A, Danko CG, Kraus WL. Enhancer transcripts mark active estrogen receptor binding sites. Genome Res. 2013; 23:1210–1223. [PubMed: 23636943]

Hawley DK, Roeder RG. Separation and partial characterization of three functional steps in transcription initiation by human RNA polymerase II. J Biol Chem. 1985; 260:8163–8172. [PubMed: 2409080]

Heuchel R, Matthias P, Schaffner W. Two closely spaced promoters are equally activated by a remote enhancer: evidence against a scanning model for enhancer action. Nucleic Acids Res. 1989; 17:8931–8947. [PubMed: 2555780]

Jiang H, Peterlin BM. Differential chromatin looping regulates CD4 expression in immature thymocytes. Mol Cell Biol. 2008; 28:907–912. [PubMed: 18039856]

Jin F, Li Y, Dixon JR, Selvaraj S, Ye Z, Lee AY, Yen CA, Schmitt AD, Espinoza CA, Ren B. A high-resolution map of the three-dimensional chromatin interactome in human Cells. Nature. 2013; 503:290–294. [PubMed: 24141950]

Kagey MH, Newman JJ, Bilodeau S, Zhan Y, Orlando DA, van Berkum NL, Ebmeier CC, Goossens J, Rahl PB, Levine SS, et al. Mediator and cohesin connect gene expression and chromatin architecture. Nature. 2010; 467:430–435. [PubMed: 20720539]

Krivega I, Dale RK, Dean A. Role of LDB1 in the transition from chromatin looping to transcription activation. Genes Dev. 2014; 28:1278–1290. [PubMed: 24874989]

Lanz RB, Bulynko Y, Malovannaya A, Labhart P, Wang L, Li W, Qin J, Harper M, O'Malley BW. Global characterization of transcriptional impact of the SRC-3 coregulator. Mol Endocrinol. 2010; 24:859–872. [PubMed: 20181721]

Larkin JD, Cook PR, Papantonis A. Dynamic reconfiguration of long human genes during one transcription cycle. Mol Cell Biol. 2012; 32:2738–2747. [PubMed: 22586273]

Lee K, Hsiung CC, Huang P, Raj A, Blobel GA. Dynamic enhancer-gene body contacts during transcription elongation. Genes Dev. 2015; 29:1992–1997. [PubMed: 26443845]

Li G, Ruan X, Auerbach RK, Sandhu KS, Zheng M, Wang P, Poh HM, Goh Y, Lim J, Zhang J, et al. Extensive promoter-centered chromatin interactions provide a topological basis for transcription regulation. Cell. 2012; 148:84–98. [PubMed: 22265404]

Li W, Notani D, Ma Q, Tanasa B, Nunez E, Chen AY, Merkurjev D, Zhang J, Ohgi K, Song X, et al. Functional roles of enhancer RNAs for oestrogen-dependent transcriptional activation. Nature. 2013; 498:516–520. [PubMed: 23728302]

Li W, Notani D, Rosenfeld MG. Enhancers as non-coding RNA transcription units: recent insights and future perspectives. Nat Rev Genet. 2016; 17:207–223. [PubMed: 26948815]

Author Manuscript Author Manuscript Author Manuscript Author Manuscript

Liu W, Ma Q, Wong K, Li W, Ohgi K, Zhang J, Aggarwal AK, Rosenfeld MG. Brd4 and JMJD6-associated anti-pause enhancers in regulation of transcriptional pause release. Cell. 2013; 155:1581–1595. [PubMed: 24360279]

Liu Z, Merkurjev D, Yang F, Li W, Oh S, Friedman MJ, Song X, Zhang F, Ma Q, Ohgi KA, et al. Enhancer activation requires trans-recruitment of a mega transcription factor complex. Cell. 2014; 159:358–373. [PubMed: 25303530]

Malik S, Roeder RG. Mediator: A Drawbridge across the Enhancer-Promoter Divide. Mol Cell. 2016; 64:433–434. [PubMed: 27814486]

Marsman J, Horsfield JA. Long distance relationships: enhancer-promoter communication and dynamic gene transcription. Biochim Biophys Acta. 2012; 1819:1217–1227. [PubMed: 23124110]

Ong CT, Corces VG. Enhancer function: new insights into the regulation of tissue-specific gene expression. Nat Rev Genet. 2011; 12:283–293. [PubMed: 21358745]

Palstra RJ, Simonis M, Klous P, Brasset E, Eijkelkamp B, de Laat W. Maintenance of long-range DNA interactions after inhibition of ongoing RNA polymerase II transcription. PLoS One. 2008; 3:e1661. [PubMed: 18286208]

Pazin MJ, Kamakaka RT, Kadonaga JT. ATP-dependent nucleosome reconfiguration and transcriptional activation from preassembled chromatin templates. Science. 1994; 266:2007–2011. [PubMed: 7801129]

Phanstiel DH, Van Bortle K, Spacek D, Hess GT, Shamim MS, Machol I, Love MI, Aiden EL, Bassik MC, Snyder MP. Static and Dynamic DNA Loops form AP-1-Bound Activation Hubs during Macrophage Development. Mol Cell. 2017; 67:1037–1048 e1036. [PubMed: 28890333]

Ptashne M. Gene regulation by proteins acting nearby and at a distance. Nature. 1986; 322:697–701. [PubMed: 3018583]

Rada-Iglesias A, Bajpai R, Swigut T, Brugmann SA, Flynn RA, Wysocka J. A unique chromatin signature uncovers early developmental enhancers in humans. Nature. 2011; 470:279–283. [PubMed: 21160473]

Ren X, Siegel R, Kim U, Roeder RG. Direct interactions of OCA-B and TFII-I regulate immunoglobulin heavy-chain gene transcription by facilitating enhancer-promoter communication. Mol Cell. 2011; 42:342–355. [PubMed: 21549311]

Schmidt D, Schwalie PC, Ross-Innes CS, Hurtado A, Brown GD, Carroll JS, Flicek P, Odom DT. A CTCF-independent role for cohesin in tissue-specific transcription. Genome Res. 2010; 20:578–588. [PubMed: 20219941]

Shang Y, Hu X, DiRenzo J, Lazar MA, Brown M. Cofactor dynamics and sufficiency in estrogen receptor-regulated transcription. Cell. 2000; 103:843–852. [PubMed: 11136970]

Siersbaek R, Madsen JGS, Javierre BM, Nielsen R, Bagge EK, Cairns J, Wingett SW, Traynor S, Spivakov M, Fraser P, et al. Dynamic Rewiring of Promoter-Anchored Chromatin Loops during Adipocyte Differentiation. Mol Cell. 2017; 66:420–435 e425. [PubMed: 28475875]

Spitz F, Furlong EE. Transcription factors: from enhancer binding to developmental control. Nat Rev Genet. 2012; 13:613–626. [PubMed: 22868264]

Spurrell CH, Dickel DE, Visel A. The Ties That Bind: Mapping the Dynamic Enhancer-Promoter Interactome. Cell. 2016; 167:1163–1166. [PubMed: 27863237]

Sun J, Nawaz Z, Slingerland JM. Long-range activation of GREB1 by estrogen receptor via three distal consensus estrogen-responsive elements in breast cancer Cells. Mol Endocrinol. 2007; 21:2651–2662. [PubMed: 17666587]

Titov DV, Gilman B, He QL, Bhat S, Low WK, Dang Y, Smeaton M, Demain AL, Miller PS, Kugel JF, et al. XPB, a subunit of TFIIH, is a target of the natural product triptolide. Nat Chem Biol. 2011; 7:182–188. [PubMed: 21278739]

Vakoc CR, Letting DL, Gheldof N, Sawado T, Bender MA, Groudine M, Weiss MJ, Dekker J, Blobel GA. Proximity among distant regulatory elements at the beta-globin locus requires GATA-1 and FOG-1. Mol Cell. 2005; 17:453–462. [PubMed: 15694345]

Visel A, Rubin EM, Pennacchio LA. Genomic views of distant-acting enhancers. Nature. 2009; 461:199–205. [PubMed: 19741700]

Author Manuscript Author Manuscript Author Manuscript Author Manuscript

Weintraub AS, Li CH, Zamudio AV, Sigova AA, Hannett NM, Day DS, Abraham BJ, Cohen MA, Nabet B, Buckley DL, et al. YY1 Is a Structural Regulator of Enhancer-Promoter Loops. Cell. 2017; 171:1573–1588 e1528. [PubMed: 29224777]

Won Jeong K, Chodankar R, Purcell DJ, Bittencourt D, Stallcup MR. Gene-specific patterns of coregulator requirements by estrogen receptor-alpha in breast cancer Cells. Mol Endocrinol. 2012; 26:955–966. [PubMed: 22543272]

Yan J, Enge M, Whitington T, Dave K, Liu J, Sur I, Schmierer B, Jolma A, Kivioja T, Taipale M, et al. Transcription factor binding in human *Cell*s occurs in dense clusters formed around cohesin anchor sites. Cell. 2013; 154:801–813. [PubMed: 23953112]

Yi P, Wang Z, Feng Q, Pintilie GD, Foulds CE, Lanz RB, Ludtke SJ, Schmid MF, Chiu W, O'Malley BW. Structure of a biologically active estrogen receptor-coactivator complex on DNA. Mol Cell. 2015; 57:1047–1058. [PubMed: 25728767]

Yun WJ, Kim YW, Kang Y, Lee J, Dean A, Kim A. The hematopoietic regulator TAL1 is required for chromatin looping between the beta-globin LCR and human gamma-globin genes to activate transcription. Nucleic Acids Res. 2014; 42:4283–4293. [PubMed: 24470145]

Zhang Y, Wong CH, Birnbaum RY, Li G, Favaro R, Ngan CY, Lim J, Tai E, Poh HM, Wong E, et al. Chromatin connectivity maps reveal dynamic promoter-enhancer long-range associations. Nature. 2013; 504:306–310. [PubMed: 24213634]

Author Manuscript Author Manuscript Author Manuscript Author Manuscript

HIGHLIGHTS

- Development of direct cell-free assays to monitor enhancer-promoter looping
- The SRC-3 coactivator governs ERα target gene enhancer-promoter looping
- E2-dependent chromatin interactions are dynamic, and involve gene body contacts
- Dynamic enhancer-promoter interaction is essential for transcriptional activation

Author Manuscript Author Manuscript Author Manuscript Author Manuscript

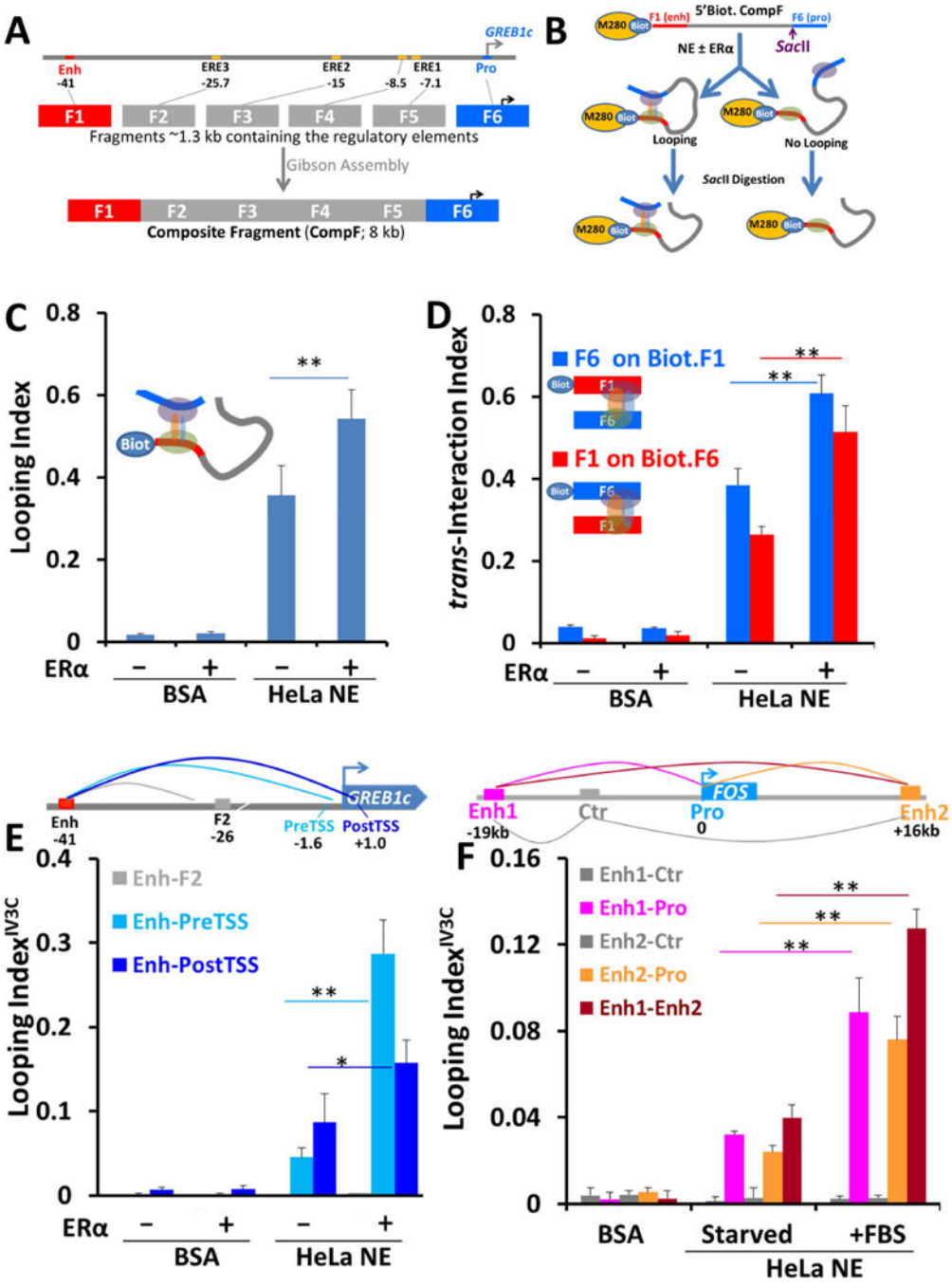


Figure 1. Development of cell-free assays to interrogate enhancer-promoter contacts (EPCs)

(A) Schematic of the human *GREB1* locus representing five regulatory elements (F1-F5) and for the *GREB1c* promoter (F6). The fragments were cloned and assembled into an 8 kb composite fragment (CompF). See also Figures S1A and S1B.

(B) Schematic of the looping assay. 5′Biot.CompF bound to streptavidin-coated M280 beads was incubated with HeLa S3 nuclear extract (NE), E2 and ATP, with or without recombinant ERα. F6 retention on the beads was quantitated by qPCR after *Sac*I digestion.

Author Manuscript Author Manuscript Author Manuscript Author Manuscript

(C) Looping assay: HeLa NE induces F6 retention on Biot.CompF, which further increases in the presence of ERα. Data are represented as mean ± standard deviation (SD) from four independent assay replicates. Inlet schematic depicts the assay. See Figures S1C and S1D for related assay.

(D) *trans*-Interaction assay: F6 enrichment on Biot.F1 (blue columns) and F1 enrichment on Biot.F6 (red columns) indicate enhancer-promoter contact. Data are represented as mean ± SD from six independent assay replicates. See also Figures S1G-S1I for related assays. Inlet schematics depict the assays.

(E) IV3C assay using *GREB1* BAC clone CTD-3138J7. The ratio of assay ligant amplicons to ligated reference BAC is represented as the "Looping Index^{IV3C}". Data are represented as mean ± SD from four independent assay replicates. Upper schematic shows qPCR primer locations relative to the transcription start site (TSS) in kb. See also Figures S2A and S2B for additional IV3C assays.

(F) IV3C assay with a *FOS* BAC clone. NE prepared from HeLa cells serum-starved for 48 hr (Starved) or 2 hr serum (FBS) stimulated was used. Ctr, a control region. See also Figure S2D. All panels in Figure 1: *p<0.01; **P<0.001; two-tail Student's t-test.

Author Manuscript
Author Manuscript
Author Manuscript
Author Manuscript

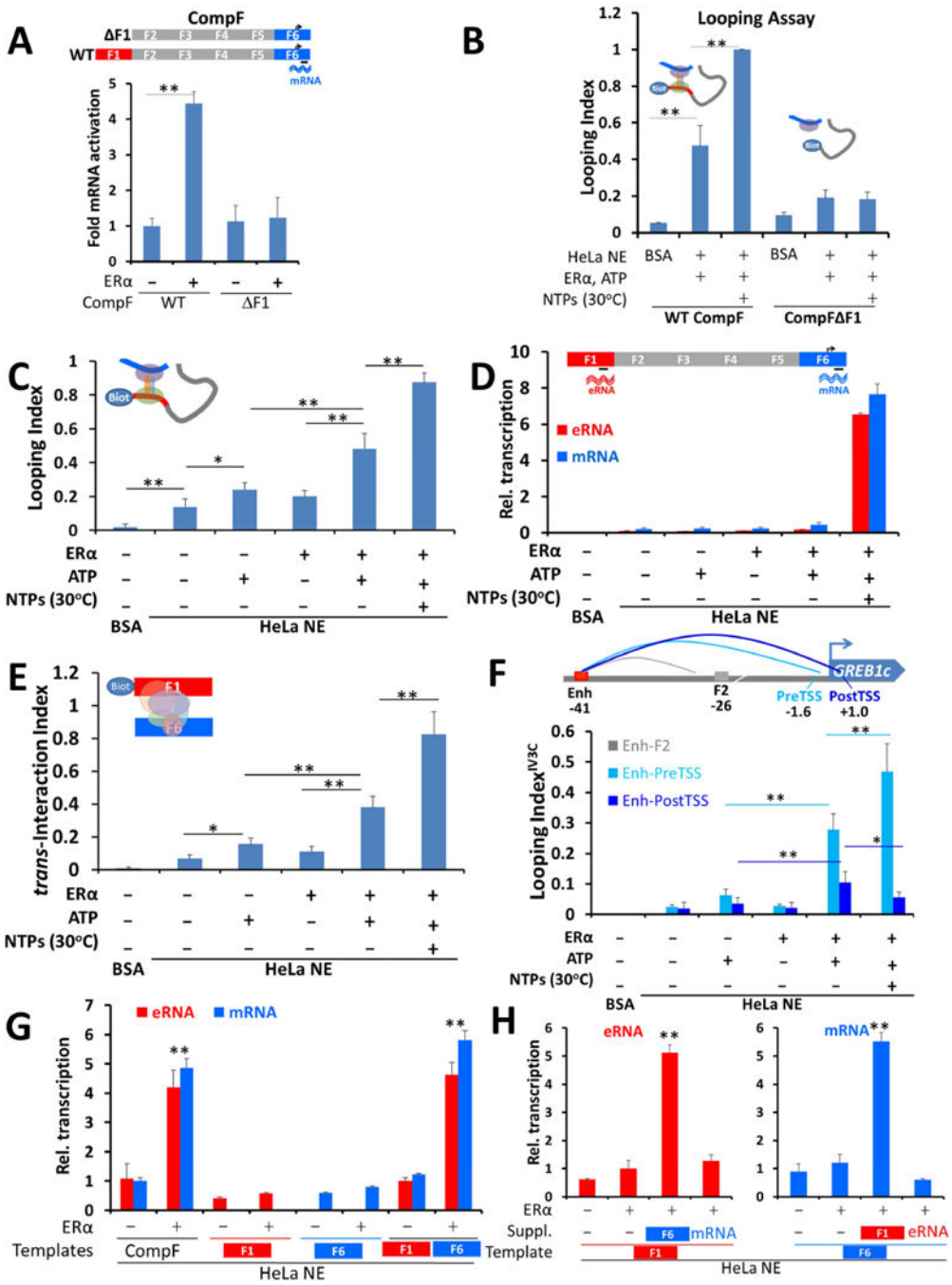


Figure 2. Cell-free assays suggest looping and transcription activation are linked together

(A) In vitro transcription (IVT) of the CompF and CompFΔF1 (schematic shown above) with HeLa NE and ERα showing that efficient mRNA production is dependent on ERα and enhancer (F1). See also Figure S2E.

(B) Looping assay with CompF and CompFΔF1 suggesting that looping of the promoter requires the enhancer. HeLa NE, ERα and ATP together represent a condition analogous to pre-initiation complex (PIC) formation; addition of 0.5 mM NTPs and shifting reactions to 30°C simulates transcription (‘transcription condition’).

Author Manuscript Author Manuscript Author Manuscript Author Manuscript

(C) Looping assay with CompF showing that maximal looping occurs under the ‘transcription’ condition (defined above). Half of the reactions were crosslinked with formaldehyde and processed for looping detection.
(D) Transcription readout of the looping assay described in Figure 2C. RNA was isolated from the other half of the reactions to quantitate both eRNA and mRNA synthesis.
(E) *trans*-Interaction assay indicating that maximal EPC occurs in the ‘transcription condition’. Reaction conditions were identical to Figures 2C and 2D, except that F6 and Biot.F1 were used as the templates.
(F) IV3C assay on the CTD-3138J7 showing that maximal enhancer (Enh)-preTSS contact occurs in the ‘transcription’ condition, while Enh-postTSS interaction was decreases under this condition. See Figure S2F for transcriptional readout of this assay.
(G) Data showing that F1 and F6 individually do not transcribe well individually, but are efficiently transcribed when present in the reaction together, either in *cis* as part of CompF, or in *trans* when co-incubated. See also Figure S2I.
(H) Transcriptional readout of *trans*-Interaction assays under ‘transcription condition’ showing that synthetic eRNA and mRNA cannot stimulate transcription on promoter and enhancer fragments, respectively, whereas coincubation of F1 and F6 allows efficient transcription on both. For all panels in Figure 2, data are represented as mean ± SD of four independent assay replicates. *p<0.01, **P<0.001; two-tail Student’s t-test.

Author Manuscript Author Manuscript Author Manuscript Author Manuscript

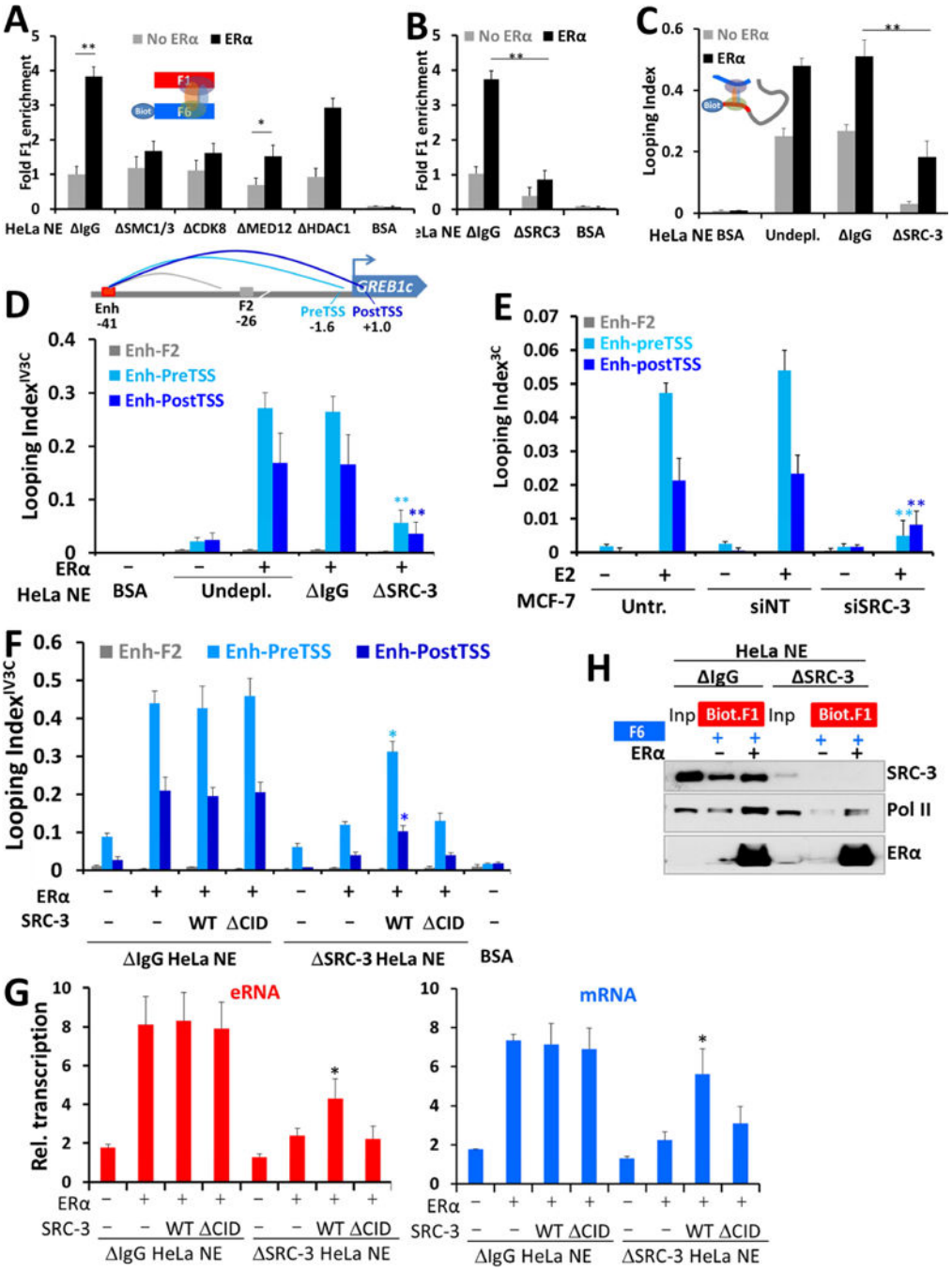


Figure 3. SRC-3 is required for looping in vitro and in MCF-7 cells

(A) *trans*-Interaction assay using immunodepleted (Δ) HeLa NE with recombinant ERα (black) or without ERα (grey), showing that loss of known looping determinants cohesin (SMC1, SMC3) and mediator (CDK8, MED12) complexes impairs EPC. ΔIgG represents NE immunodepleted with normal rabbit IgG. See also Figure S3A.

(B) *trans*-Interaction assay with F1 and Biot.F6 showing immunodepletion of SRC-3 impairs EPC. See also Figure S3B.

Author Manuscript Author Manuscript Author Manuscript Author Manuscript

(C) Looping assay on CompF showing that immunodepletion of SRC-3 impairs looping. Undepl.: undepleted NE.
(D) IV3C assay on CTD-3138J7 showing that immunodepletion of SRC-3 reduces EPC.
(E) 3C assay in MCF-7 cells after 60 minutes of E2 treatment showing that siRNA-mediated depletion of SRC-3 abolishes E2-inducible EPC at the *GREB1* locus. Untr.: untransfected; siNT: non-targeting control siRNA; siSRC-3, SRC-3 targeting siRNA. See also Figures S3E, S3F for related controls.
(F) IV3C assay on the *GREB1* BAC clone CTD-3138J7 showing that recombinant WT, but not the ΔCID mutant of SRC-3, can partially rescue looping defect due to SRC-3 depletion. See also Figures S3H, S3I for controls.
(G) IVT assays on the *GREB1* BAC clone CTD-3138J7 showing that *GREB1* eRNA and mRNA activation by ERα is significantly reduced in SRC-3 immunodepleted HeLa NE, which can partially be rescued by supplemental WT SRC-3 protein, but not by the ΔCID mutant.
(H) Combination pulldown of F6 and biotinylated F1 (Biot.F1) showing reduced recruitment of the largest subunit of RNA Pol II to the enhancer-promoter combination in absence of SRC-3, both with and without recombinant ERα. Inp indicates 3% input NE. Panels A-G: data are represented as mean ± SD from four independent assay replicates.*$p<0.01$; **$p<0.001$; Student's t test.

Author Manuscript Author Manuscript Author Manuscript Author Manuscript

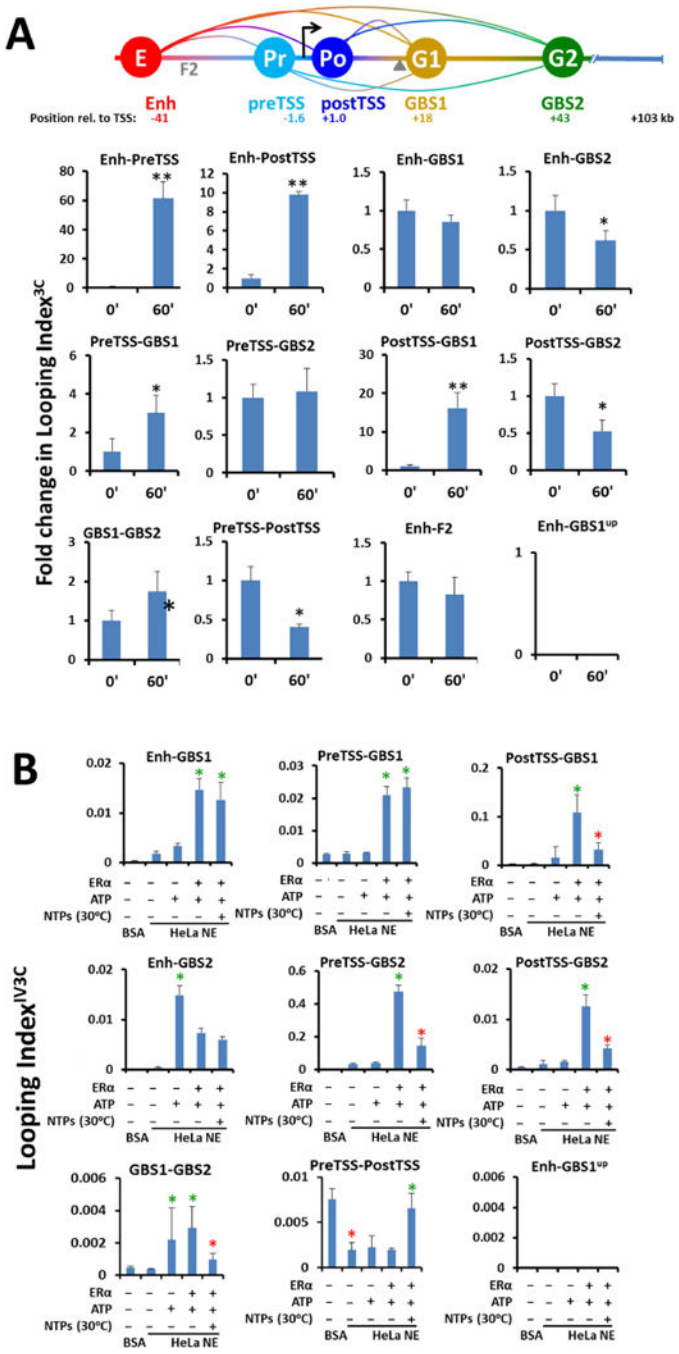


Figure 4. *GREB1* enhancer and promoter contact two intragenic SRC-3 binding sites in MCF-7 cells and in vitro

(A) 3C assays identify various pairs of contacts within the *GREB1* gene in hormone-deprived MCF-7 cells (0′) and after 60 minutes of 100 nM E2 treatment (60′). The Looping Index^{3C} was normalized to the ligated *Pst*I-cut BAC clone CTD-2563K11. The values for each interaction pair in untreated (0′) cells were set to 1, resulting in "Fold-change in Looping Index^{3C}". Two gene-body SRC-3 binding sites, GBS1 and GBS2, were assayed as indicated. Interrogated pairs of contacts are shown. E, Pr, Po, G1 and G2 represent Enhancer, preTSS promoter, postTSS promoter, GBS1 and GBS2, respectively. Location of

Author Manuscript Author Manuscript Author Manuscript Author Manuscript

control sequence F2 is indicated. Grey arrow near G1 (GBS1) indicates a control sequence (GBS1^{up}). See also Figure S1L.

(B) IV3C assays using the *GREB1* BAC clone CTD-2563K11 showing contacts of enhancer (Enh) and promoter (preTSS and postTSS) with GBS1 and GBS2 in vitro. Green asterisk (*) signifies gain in contact over NE alone, while red asterisk (*) signifies loss of contact during transcription. In all panels, *p<0.01, **p<0.001 (two-tail Student's t-test of four independent assay replicates).

Author Manuscript Author Manuscript Author Manuscript Author Manuscript

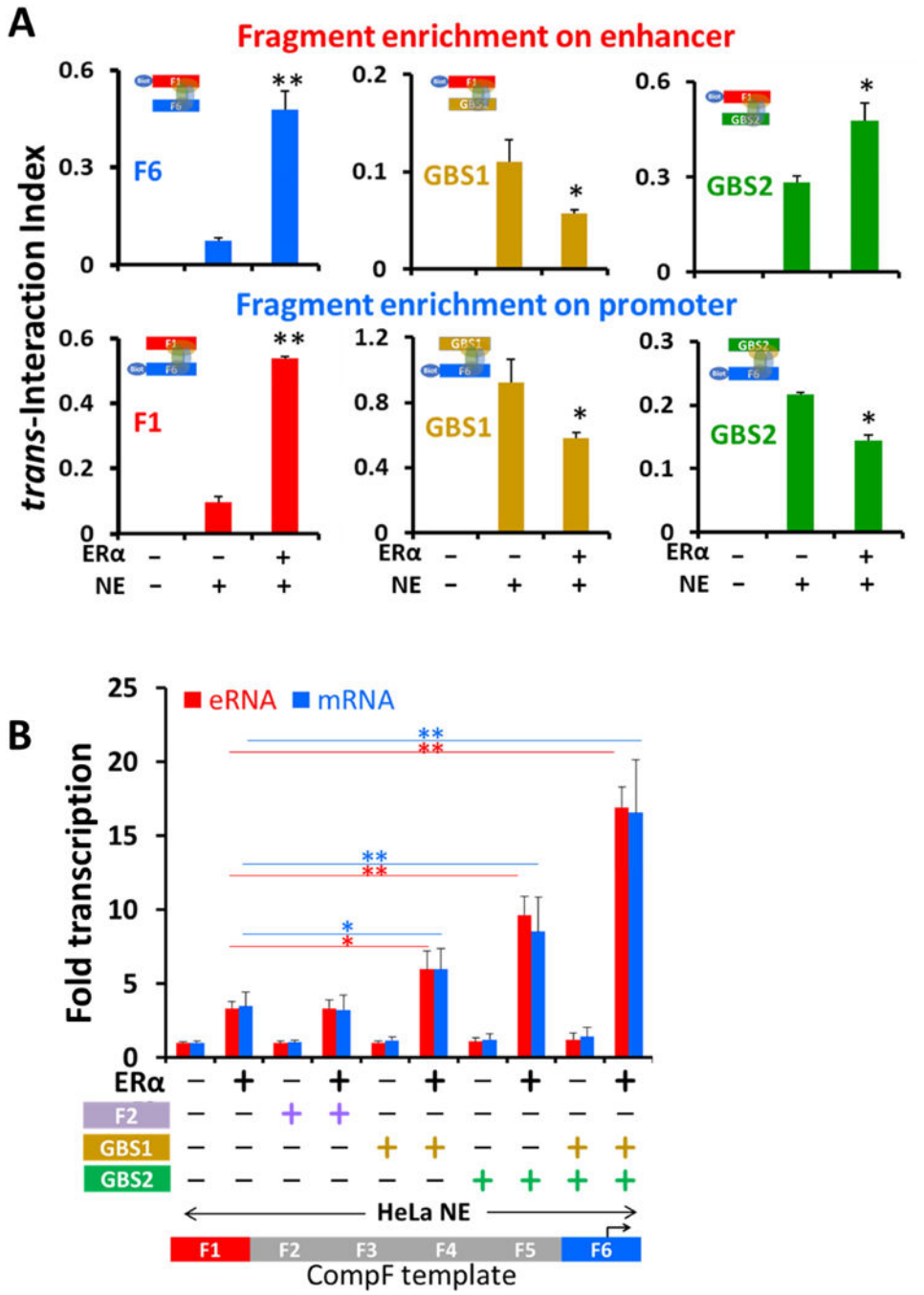


Figure 5. GBS1 and GBS2 stimulate cell-free transcription

(A) *trans*-Interaction assays showing that GBS1 and GBS2 physically interact with both enhancer and promoter in vitro using biotinylated enhancer (top panel) or promoter (bottom panel).

(B) IVT assays on CompF without or with ERα supplemented with equimolar F2, GBS1, GBS2 or GBS1+GBS2 revealed that GBS1 and GBS2 individually or together, but not F2, stimulate transcription at enhancer and promoter. See also Figures S4B, S4C. For panels in

this figure, data are represented as mean ± SD of four independent assay replicates; *p<0.01, **p<0.001.

Author Manuscript Author Manuscript Author Manuscript Author Manuscript

Author Manuscript Author Manuscript Author Manuscript Author Manuscript

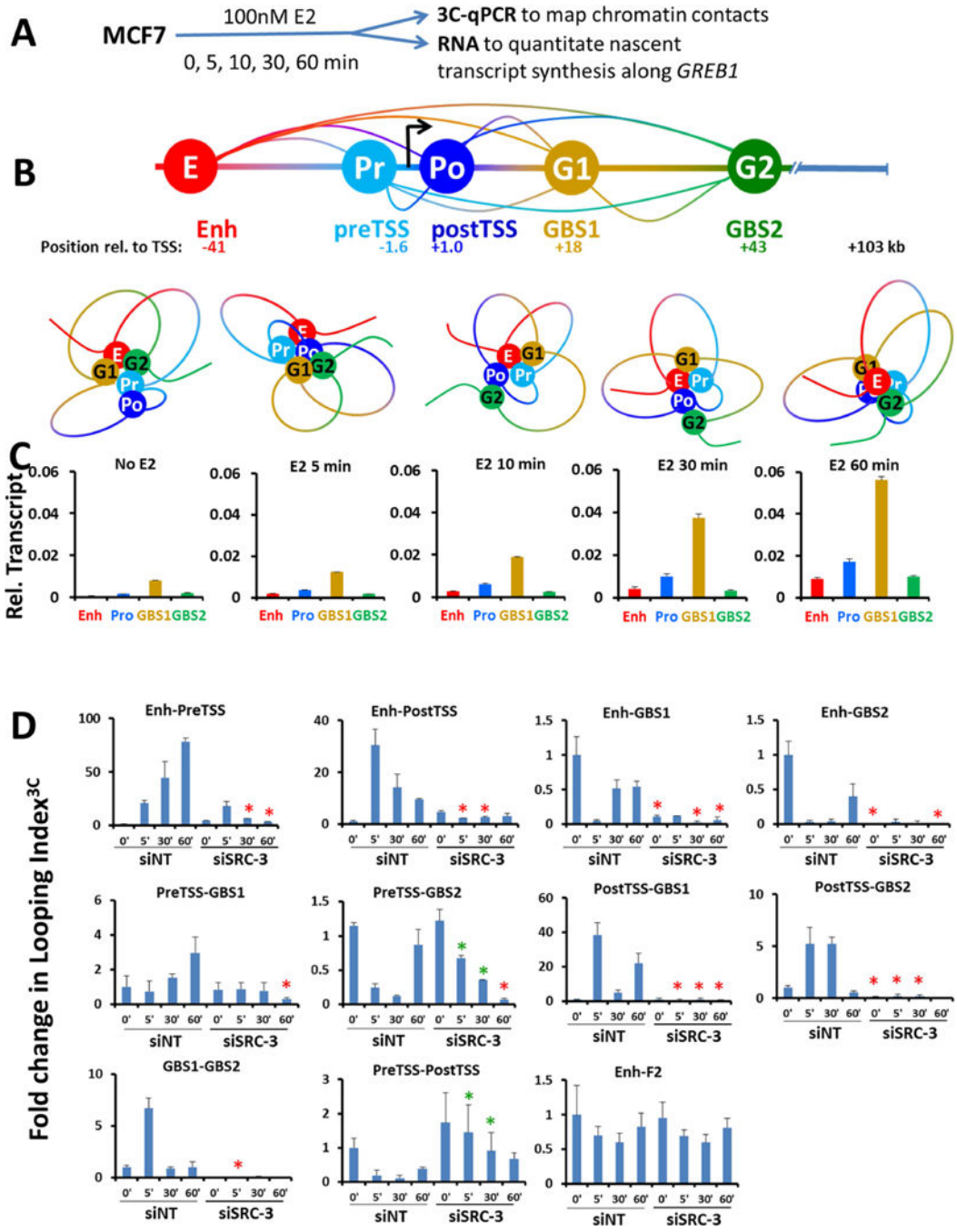


Figure 6. Chromatin interaction landscapes dynamically resonate with E2-induced transcription

(A) Schematic of the experiment. Hormone-deprived (0) or E2-treated MCF-7 cells (100 nM E2 for 5, 10, 30 and 60 minutes) were subjected to 3C-qPCR or RT-qPCR analyses.

(B) Connectivity maps showing changes in interactions over 1 hr of E2 treatment as measured by 3C assays. Fold-change in Looping Index^{3C} at 5, 10, 30 and 60 min after E2 treatment for each contact was calculated as the ratio to the respective values in untreated (0′) cells. The values for fold-change in Looping Index^{3C} (see also Figure S5) at various time points were used to manually construct connectivity maps. No significant contacts were

Author Manuscript Author Manuscript Author Manuscript Author Manuscript

identified for circle pairs that do not touch each other. Schematic of the connecting points is shown above.

(C) Plots for Nascent transcript levels at enhancer (Enh), postTSS (Pro), GBS1 and GBS2 at the indicated time points are shown underneath the corresponding connectivity map (B). Y-axis represents relative nascent transcript level (Rel. Transcript) normalized to *ACTB* mRNA. Data are represented as mean ± SD of six qPCR reactions representing two biological replicates.

(D) Fold-change in Looping Index^{3C} plots for interrogated interactions in untreated (0′) and E2-treated (5′, 30′, 60′) MCF-7 cells that were transfected with either non-targeting siRNA (siNT) or SRC-3 targeting siRNA (siSRC-3) for 72 hr prior to E2 treatment. Data are represented as mean ± SD of four independent assay replicates (three qPCR reactions each). *$p<0.01$ (two-tail Student t-test) signifies loss of contacts (red asterisks) or gain of contacts (green asterisks) upon SRC-3 knockdown.

Author Manuscript Author Manuscript Author Manuscript Author Manuscript

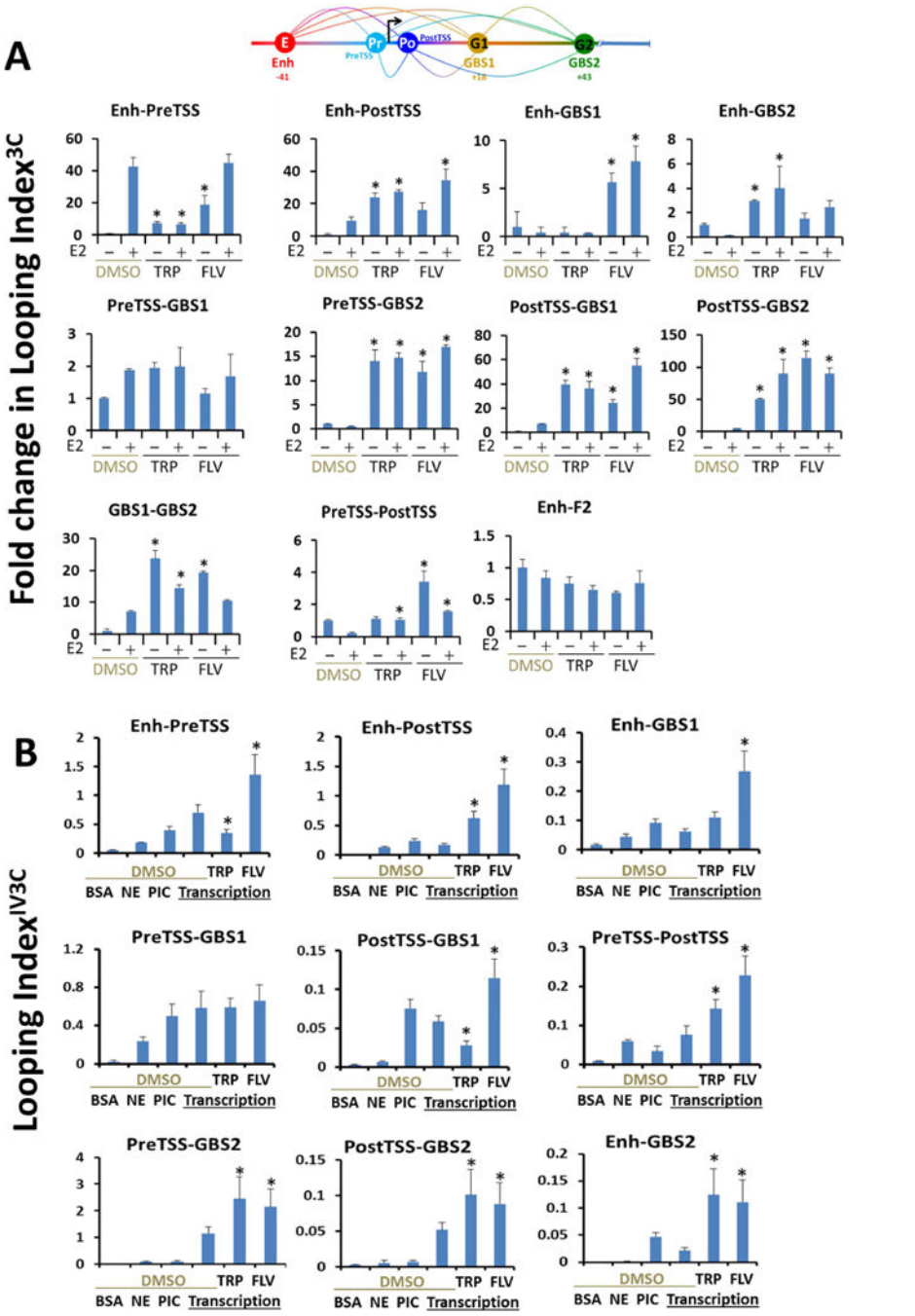


Figure 7. RNA Pol II transcription inhibition 'freezes' chromatin contacts

(A) 3C assays for *GREB1* locus chromatin interactions. MCF-7 cells were treated with (+) or without (−) 100 nM E2 for 60 min. Cells were pre-treated with transcription inhibitors triptolide (TRP; 1 μM) or flavopiridol (FLV; 1 μM) for 60 min before E2 treatment. Cells with no inhibitors received equal volumes of the DMSO vehicle. See also Figure S10A. Data are represented as mean ± SD. *p<0.01 for change in contact efficiencies over DMSO-treated cells, based on two tail Student t-test of four independent assay replicates.

Author Manuscript Author Manuscript Author Manuscript Author Manuscript

(B) IV3C assays using the *GREB1* BAC clone CTD-2563K11 to test effects of transcription inhibitors on looping interactions in vitro (Looping Index^{IV3C}). DMSO, TRP and FLV were added to the buffer and BAC template prior to addition of NE and recombinant ERα. PIC (pre-initiation complex): NE plus ATP and ERα; Transcription: PIC plus 0.5 mM NTPs with incubation at 30°C for further 25 min. See also Figure S10B. Data are represented as mean ± SD. *p<0.01 for change in contact efficiencies over DMSO-treated transcription condition, based on two tail Student t-test of four independent assay replicates.